Long-term Variability of solar eruptive events

Nat Gopalswamy
NASA Goddard Space Flight Center, Greenbelt, MD 20771, USA

Space Climate 7 Symposium Canton Orford July 8-11, 2019

Major Parts

- Historical Introduction to CMEs
- Connection to Sunspots
- Connection to Polarity Reversal

A Brief History: Solar and Interplanetary Milestones

- 1634: Variation in geomagnetic field (Gellibrand, in Fleming 1939)
- 1740s: geomagnetic disturbances correlated with aurora (Graham, Celsius, Hirorter)
- 1800s: Humboldt coins “magnetic storm”, sets up worldwide magnetic observatories
- 1859: R. C. Carrington observes a flare from a sunspot region followed by the the great storm of 1859
- 1892: G. Fenyi finds prominence eruptions as fast as several 100 km/s
- 1908: G. E. Hale discovers magnetic field in sunspots and sets up worldwide H-alpha flare patrol (1931)
- 1943: H. W. Newton estimates the corpuscular stream extent of ~90°
- 1946: S.E. Forbush reports energetic particles associated with flares (Forbush decrease in 1937)
- 1947: R. Payne-Scott discovers Type II radio bursts suggesting connection to filament eruption
- 1953: T. Gold proposes interplanetary shock to explain sudden commencement
- 1957: A. Boischot discovers moving type IV bursts (radio-emitting plasmoids)
- 1960: Pioneer 5 detects Forbush decrease outside Earth’s magnetosphere - due to flare plasma
- 1962: Mariner II detects an interplanetary shock; Gold’s conceptual CME
- 1971: OSO-7 observes the first white-light CME

G 2016 review

Prominence Eruptions Known by the End of 19th Century

Prominence emits in Ku band (17 GHz)!
Nobeyama Radioheliograph
(Gopalswamy et al. 1998)

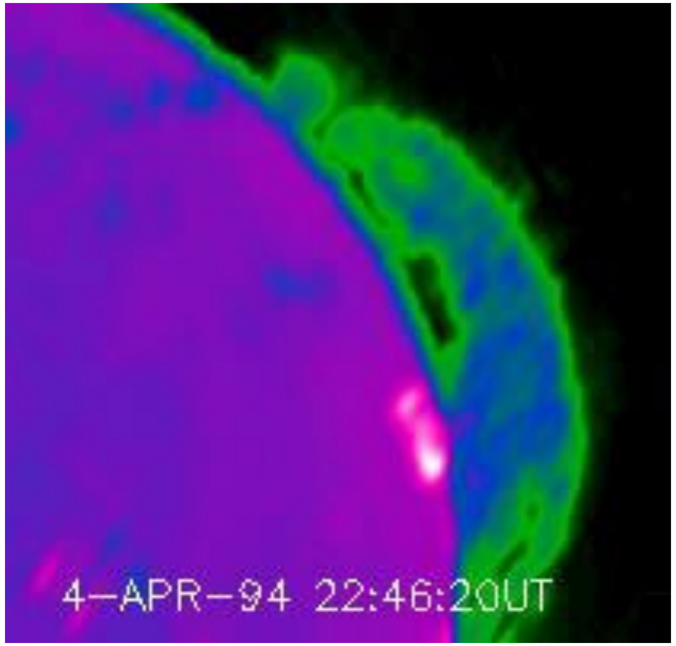

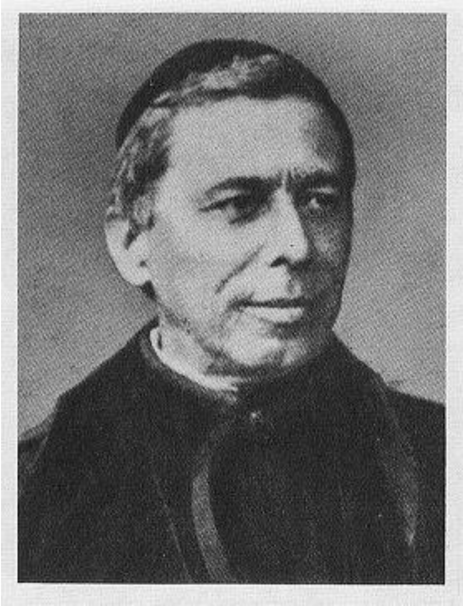

Angelo Secchi

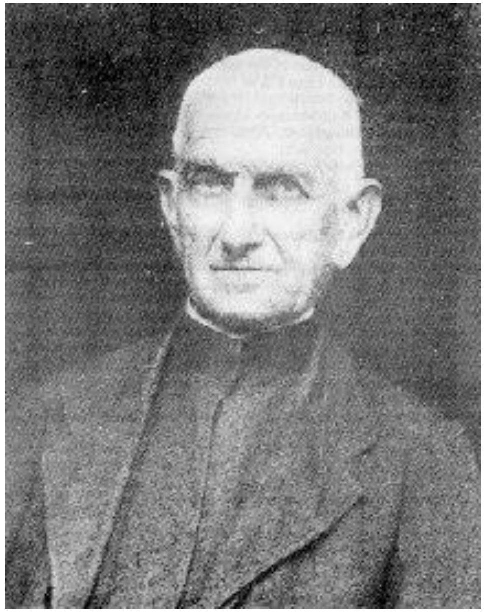

Gyula Fenyi

1868: Janssen & Lockyer demonstrated that prominences could be viewed outside of eclipses using spectroscope

1871: Secchi classified active and quiescent prominences
1892: Fenyi: Prominence eruptions have speeds exceeding 100s of km/s

Ruby Payne-Scott
1912 – 1981

Radio Bursts Reveal Matter Leaving the Sun

The whole pattern drifts; 140 MHz in 6 min → df/dt = 0.4 MHz/s
"…the derived velocities are of the same order as that of prominence material…"

Payne-Scott et al. 1947, Nature 260, 256

Plasma density
5.0 x10^8 cm^{-3}

1.2 x10^8 cm^{-3}

0.4 x10^8 cm^{-3}

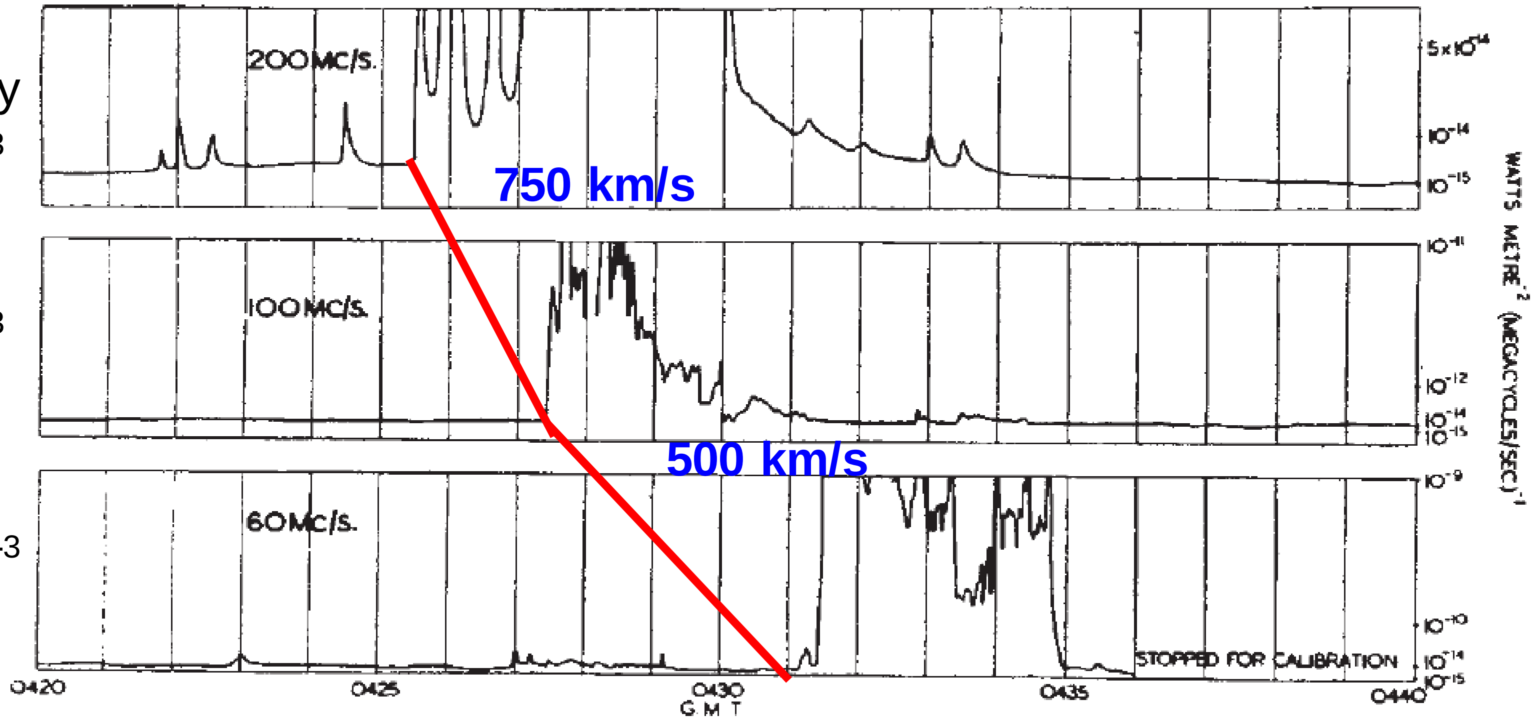

Large outburst of March 8, 1947

- classified as type II radio bursts caused by ~10 keV electrons accelerated in MHD shocks (Uchida 1960)

A moving type IV burst observed by the Culgoora Radioheliograph in Australia

~MeV electrons trapped in magnetic structures emitting at 80 MHz
Originally discovered by A. Boischot in 1957

350 km/s

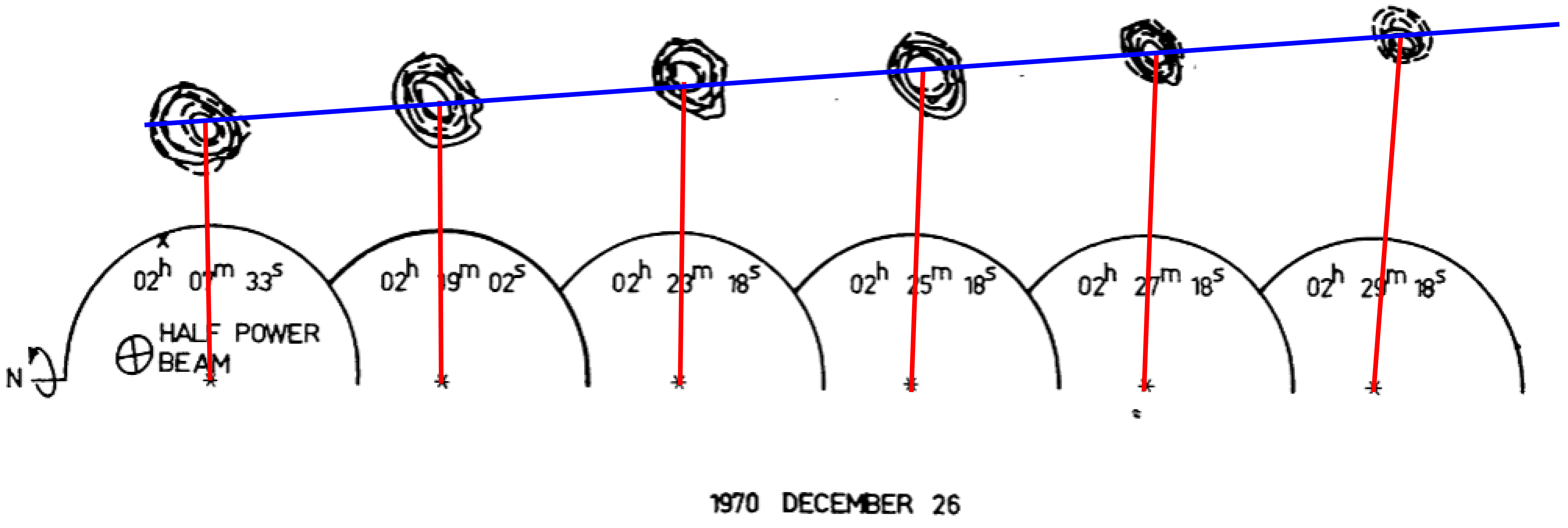

Schmahl 1972

Theory

"… magnetic clouds may be ejected from a magnetic field with velocities as high as the Alfven wave velocity"

Parker (1957)

Eugene Parker
(1927 -)

Shocks in the IP medium

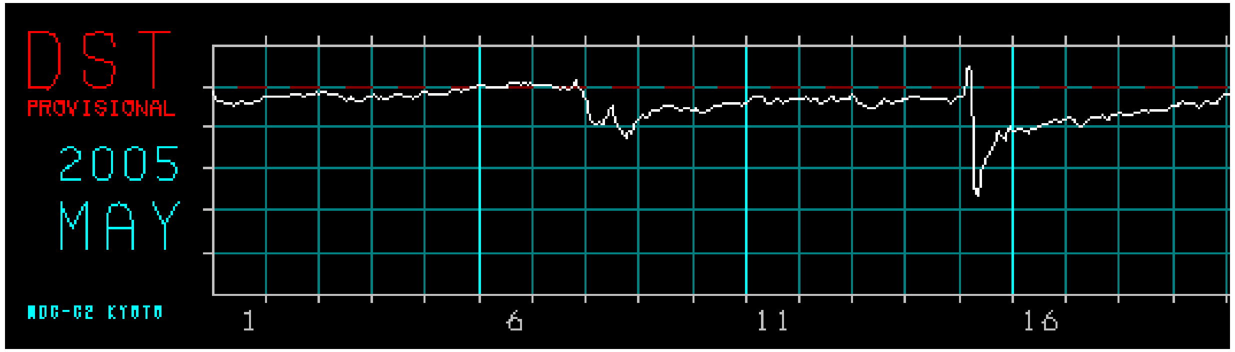

1953: Gold proposed Interplanetary shock to explain the Sudden Commencement

T. Gold (1920 – 2004)

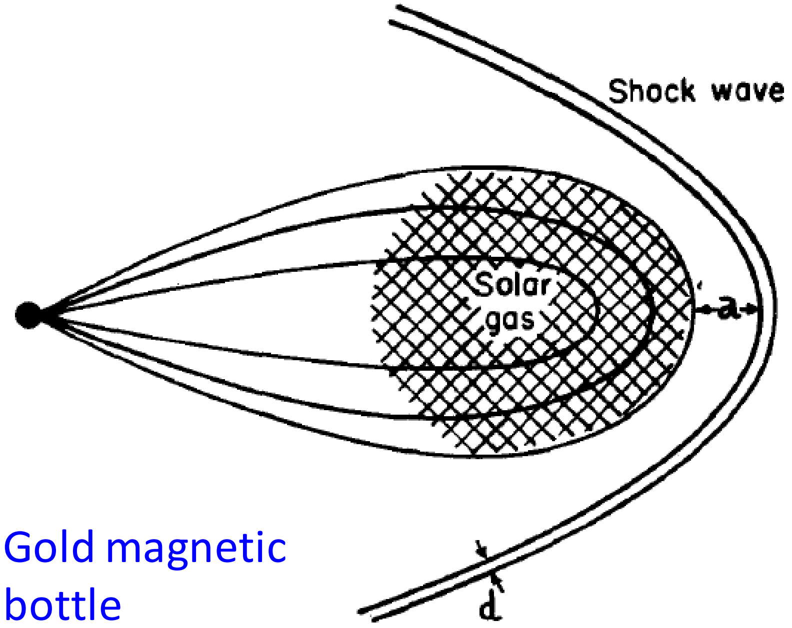

Gold magnetic bottle

1962: "Idealized configuration in space, showing solar plasma cloud, the drawn-out field and the shock wave ahead"

MHD shock theory: de Hoffmann & Teller 1950
Parker applied it to interplanetary shocks in 1963

High Velocity Magnetized Plasma from the Sun

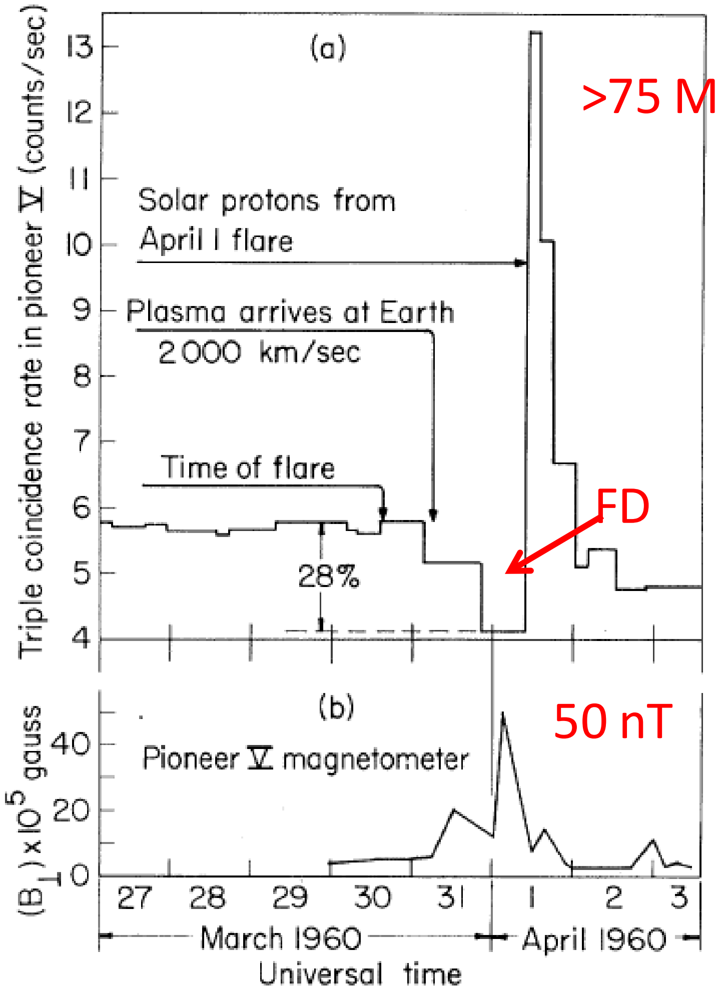

Fan, Meyer, Simpson, 1960 Phys Rev Lett

Pioneer 5
launch: 3/11/1960

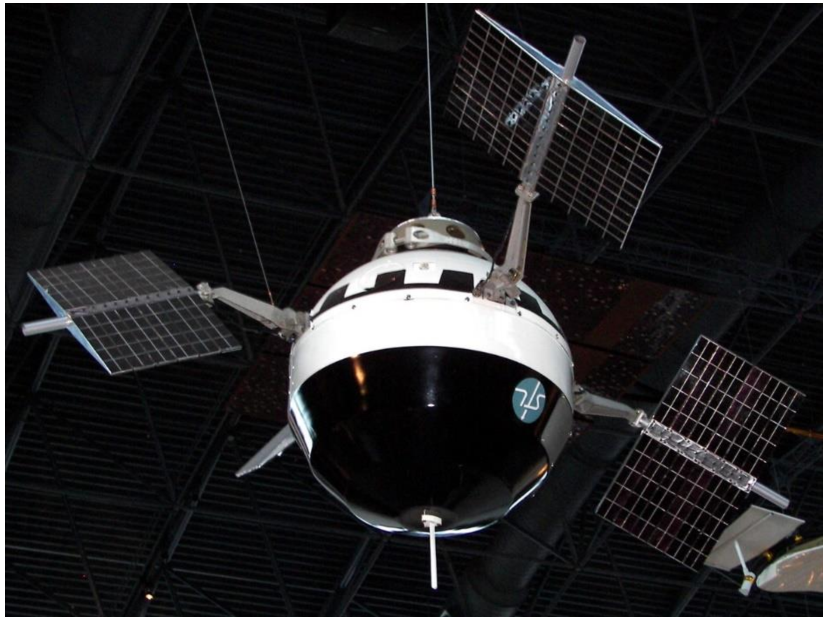

"…we believe these Pioneer V results provide the most direct evidence to date for the existence of conducting gas ejected at high velocity from solar flares"

FDs were initially thought to be due to
The ring current because of the temporal association

Mariner 2 Detects IP Shock

C P Sonett (1924 -2011)

Mariner II

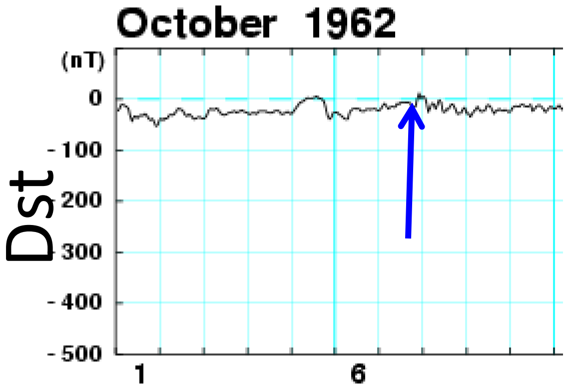

1962/10/07 15:46 UT

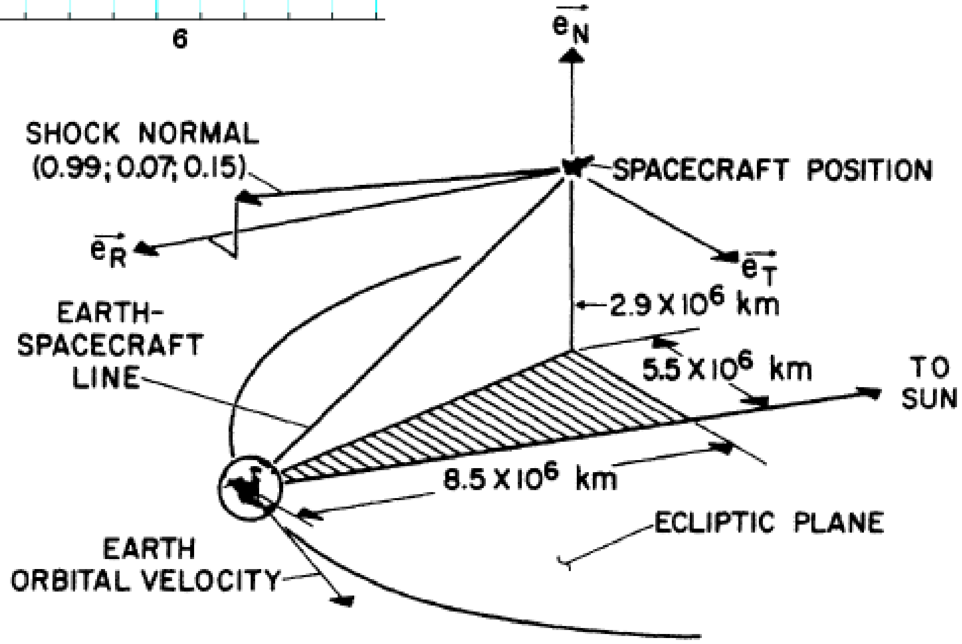

FIG. 1. Geometry of the Mariner II orbit on 7 October 1962. The shock normal direction computed from the change in the magnetic field is indicated. $\vec{e}_R, \vec{e}_N, \vec{e}_T$ are unit vectors defining a coordinate system along the radius vector from the sun, toward the ecliptic north pole, and along $\vec{e}_N \times \vec{e}_R$, respectively.

IP shock followed by a Sudden Commencement 4.7 h later - confirmed Gold's (1953) suggestion

H. E. Taylor (1969): statistical study of IP shocks and SCs

Sonett et al., 1964, Phys. Rev. Lett

CMEs Waiting to be Discovered…

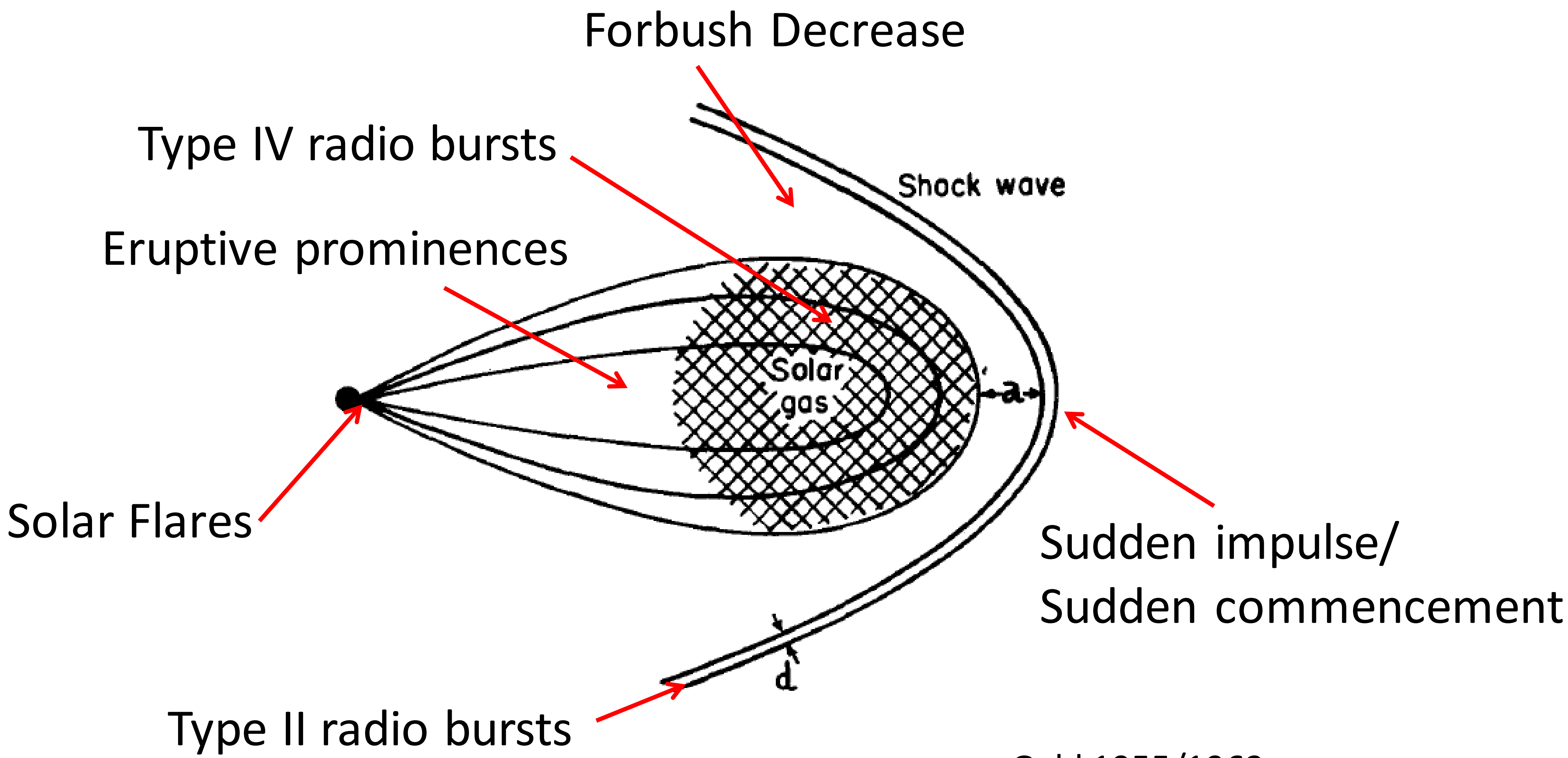

Gold 1955/1962

The first white-light CME from OSO-7

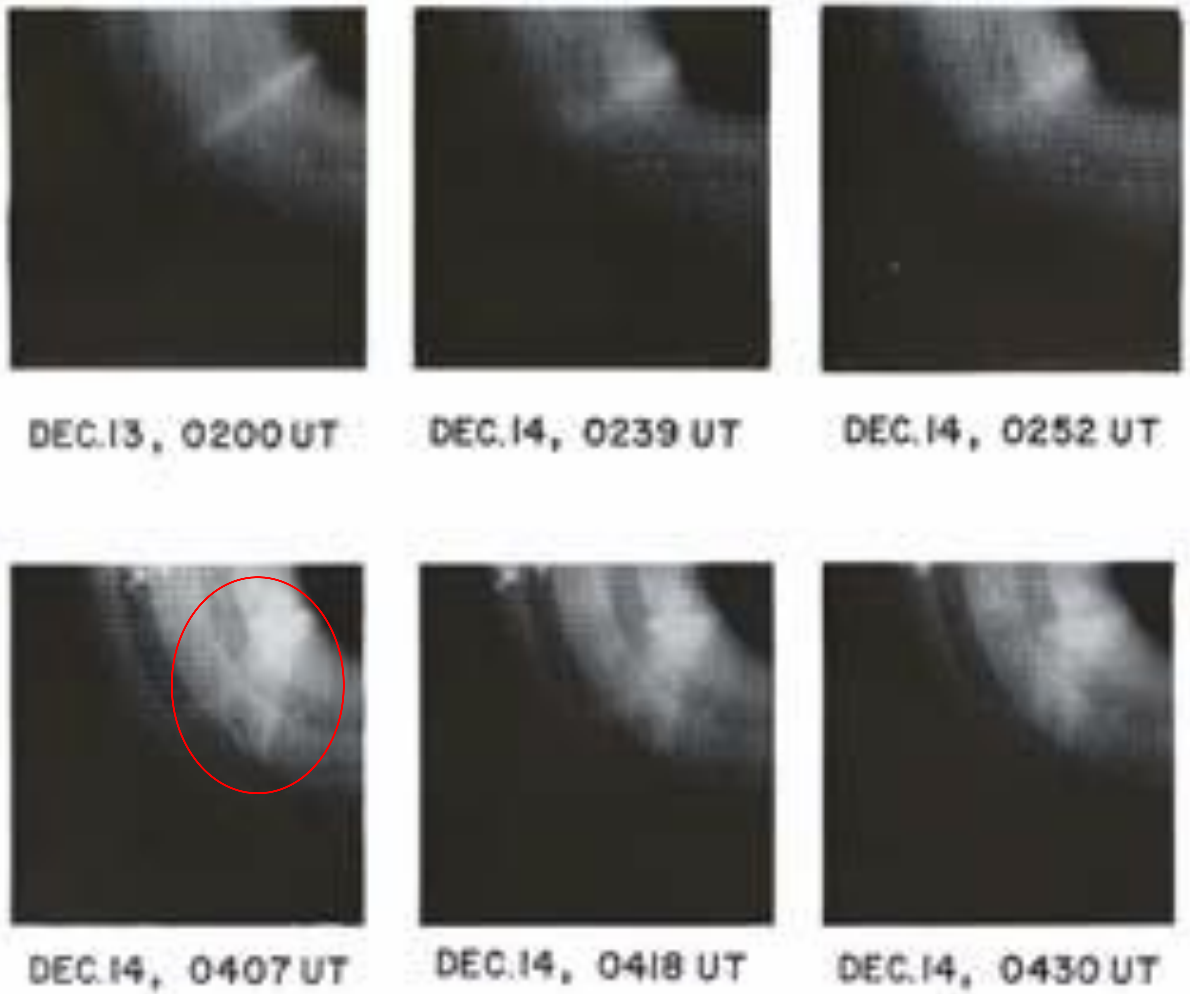

Koomen et al. 1972; Brueckner et al. 1972; Tousey, 1973
Fast coronal transient (1100 km/s) of 1971 Dec 14
OSO-7 observed 23 CMEs in all

Skylab (110 CMEs), Solwind on P78-1 (1607),
Coronagraph/Polarimeter on SMM (1206)
SOHO/LASCO , STEREO/SECCHI (~30,000)
MLSO Mark IV K -Coronameter

NASA's OSO-7

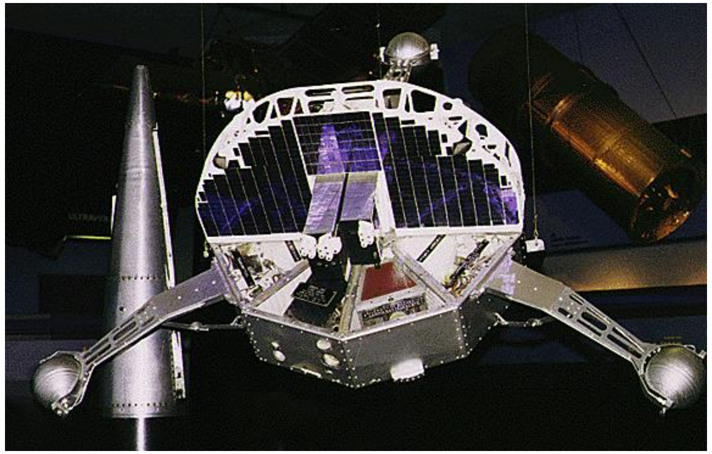

September 29, 1971 – July 9, 1974

David Roberts, the NRL electronics technician responsible for day-to-day operations noticed the bright patch and thought his camera had failed.

SOHO: Observations over Two Solar Cycles

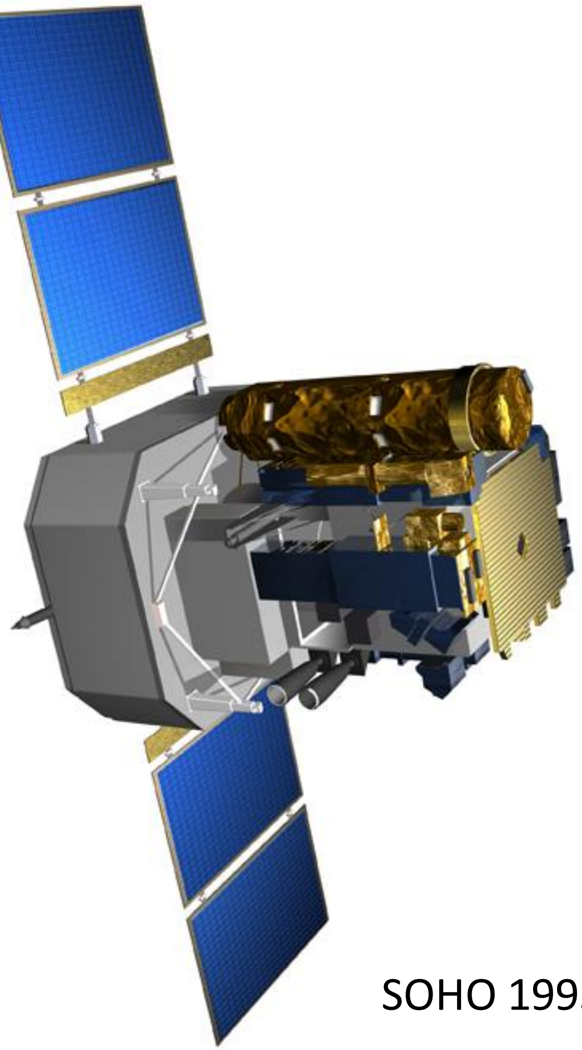

SOHO 1995 -

About 30,000 CMEs by the end of 2018
721 Full halo CMEs
2 CMEs with speed > 3000 km/s (highest 3600 km/s)
Higher CME rate
High-latitude CMEs related to polarity reversal
Cycle to cycle comparison
Flux-rope morphology discovered
Coronal dimming as indicator of CME flux rope
Detection of white-light shocks
CME deflection by coronal holes
CME Cannibalism (SOHO-Wind)
Flare-CME coupled evolution
Flare-CME connection: IP signatures (SOHO-ACE)
Automatic detection (CacTUS, SEEDS, ARTHEMIS, CORIMP)
CME arrival prediction models, simulations
Two extreme events

A CME Impacting Earth

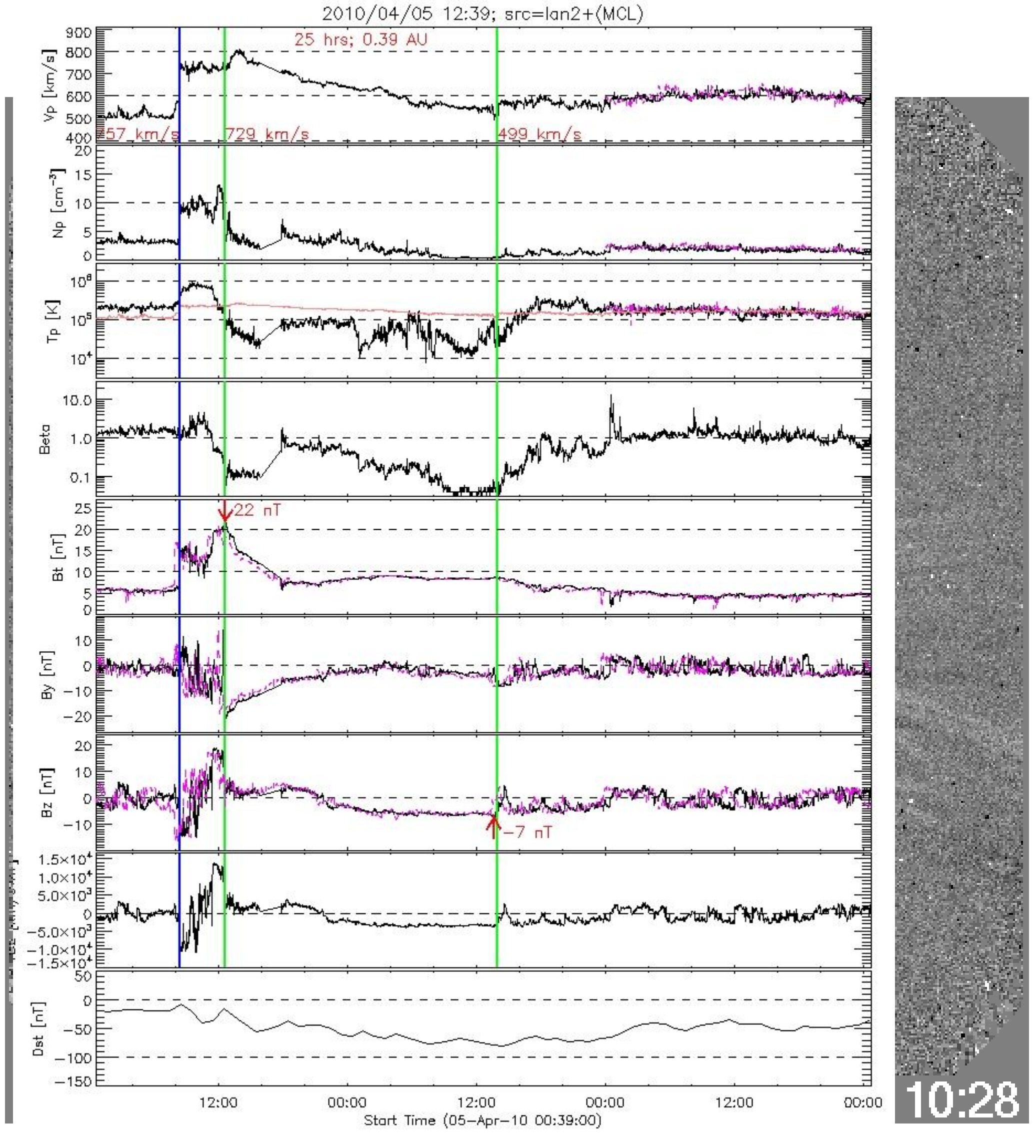

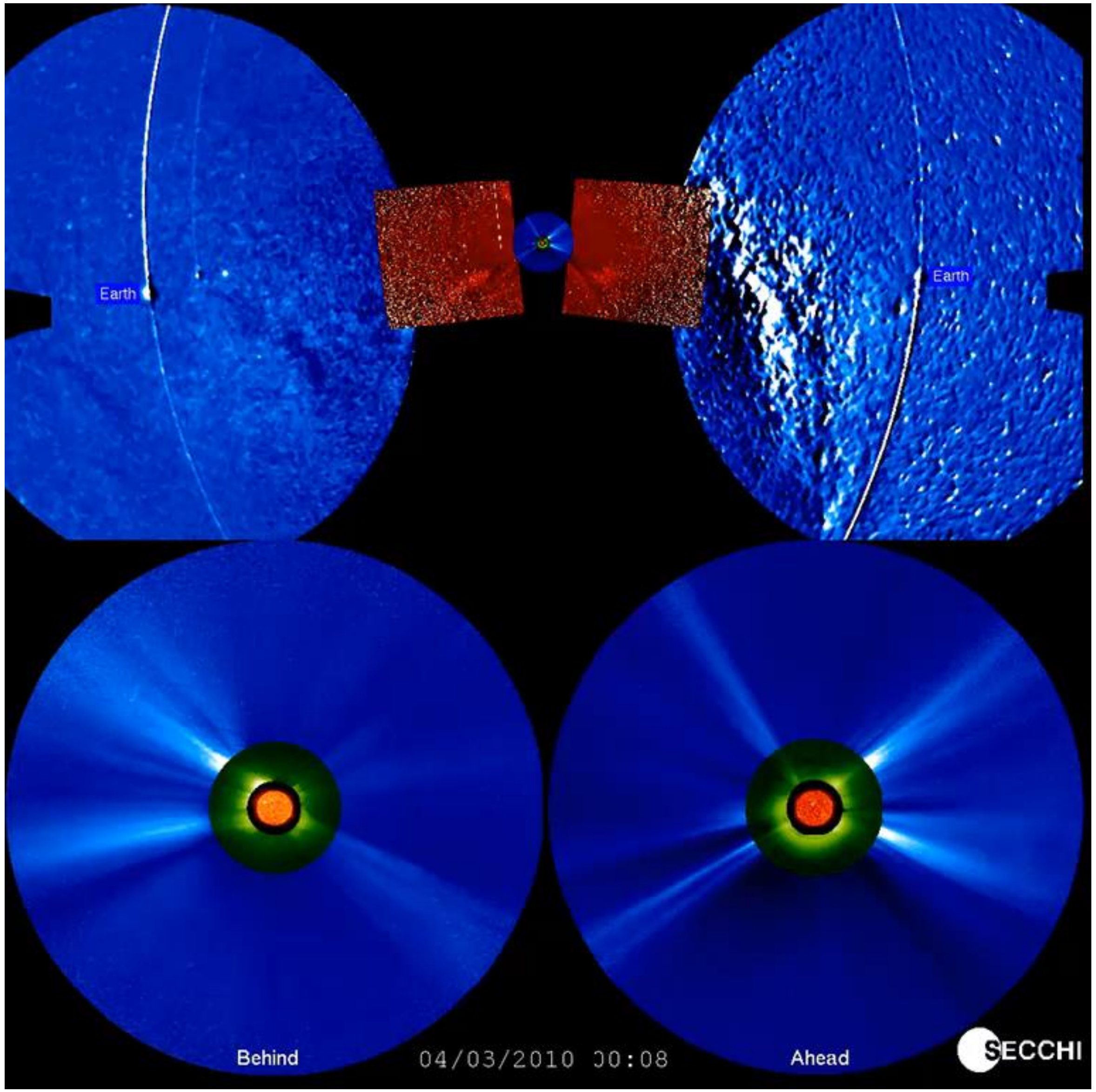

Natural Hazard: Geomagnetic Storms & SEPs

59% of reporting S/C and 18% of onboard instrument groups reported problems

Barbieri & Mahmot 2004

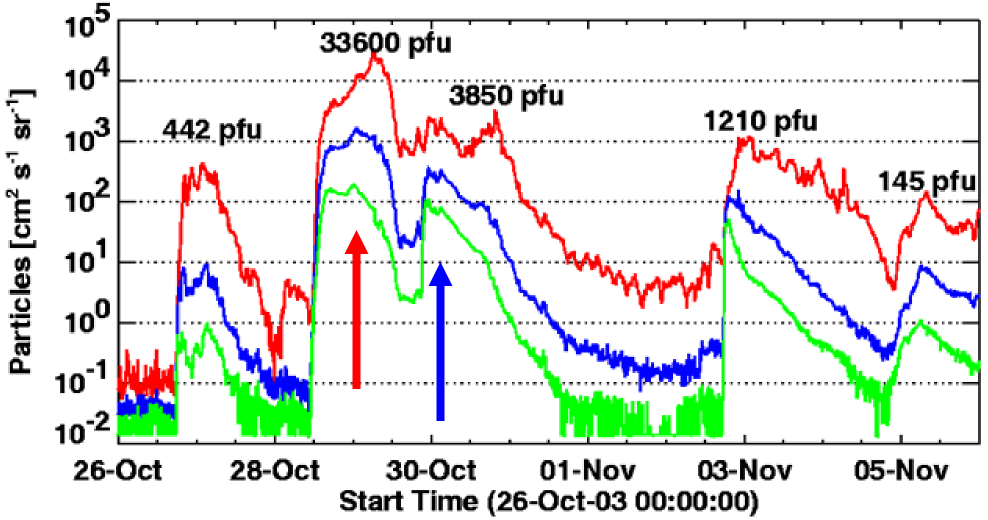

Two halo CMEs: 10/28 and 10/29 2003

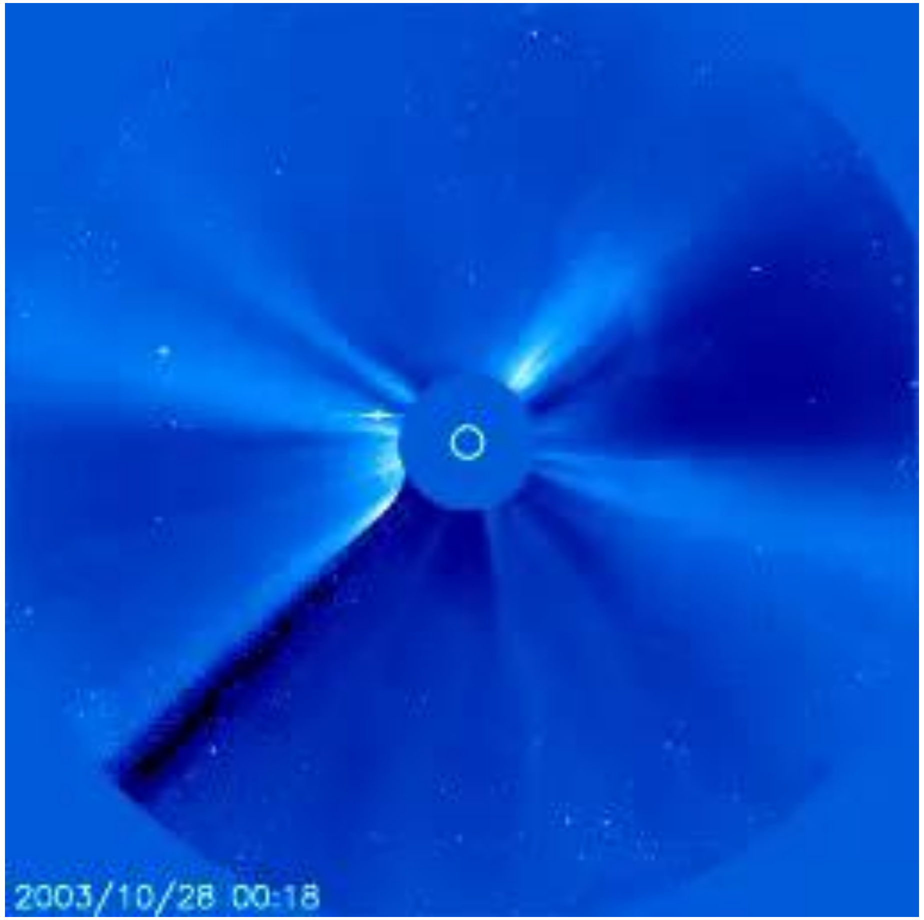

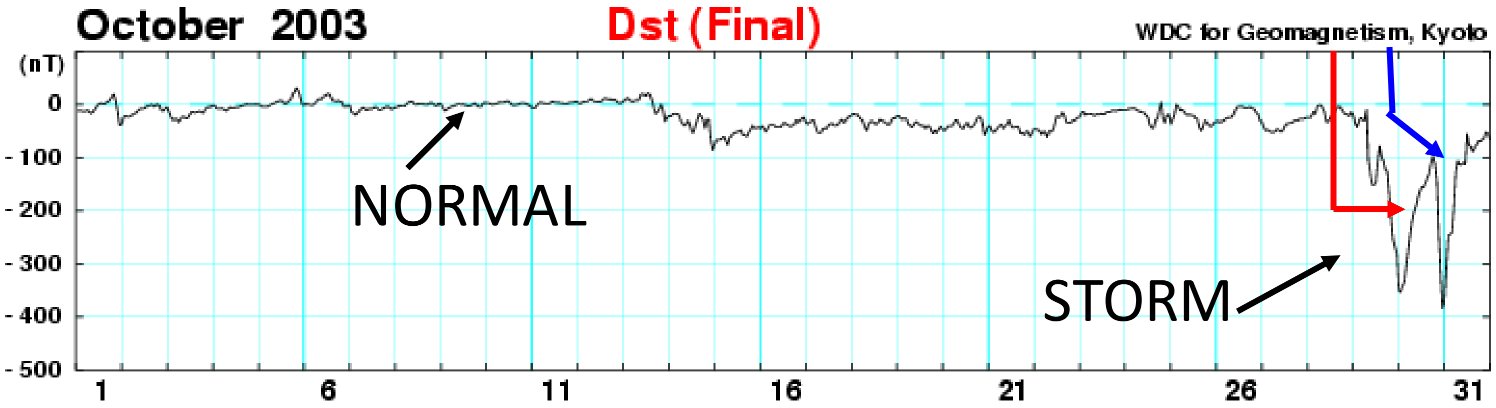

Transformer oil heated by 10^o in Sweden; 50,000 people in Malmo had power blackout

SOHO/LASCO

Eruption Geometry

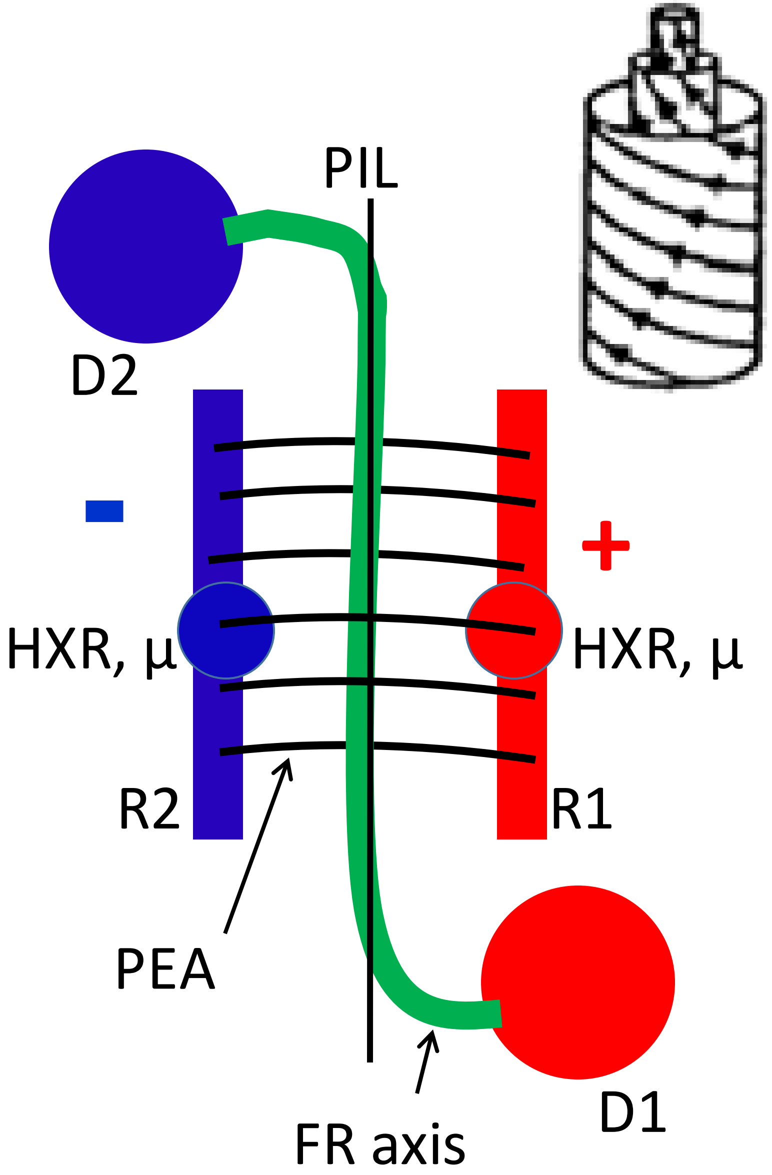

Gopalswamy 2009

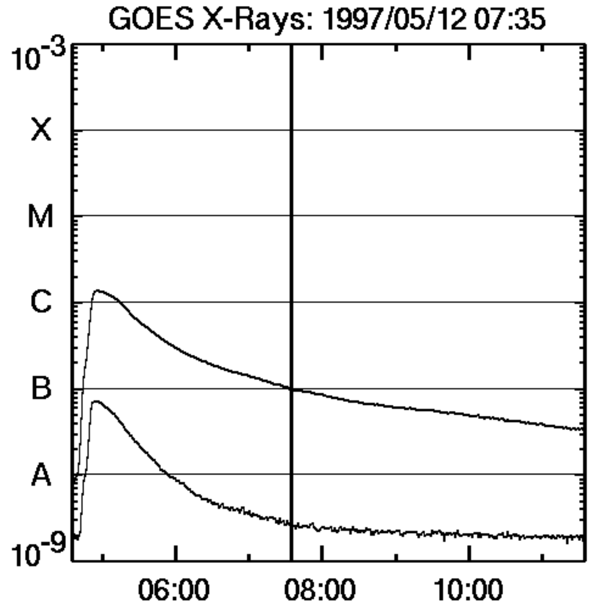

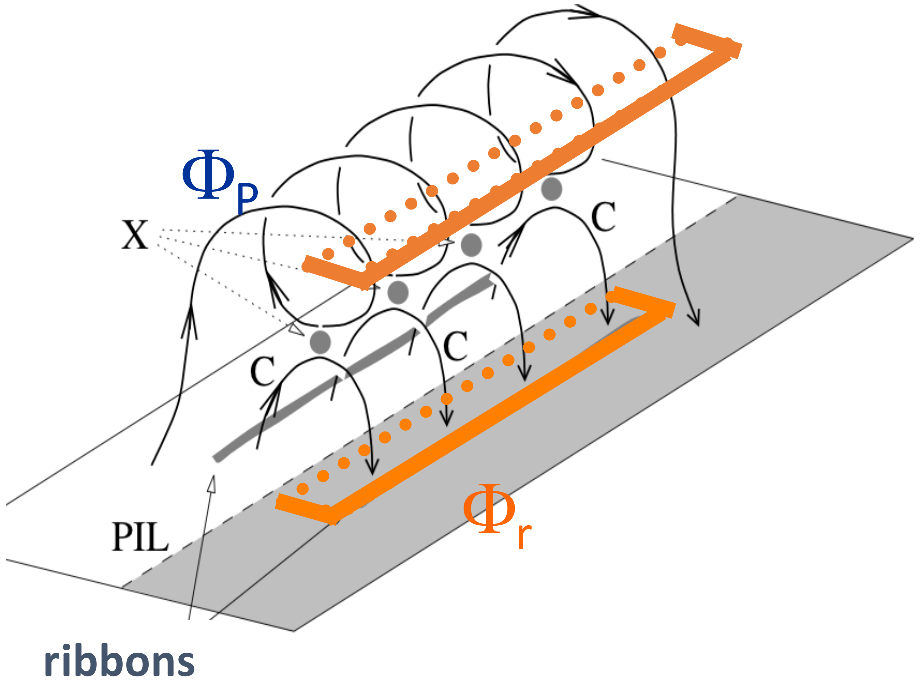

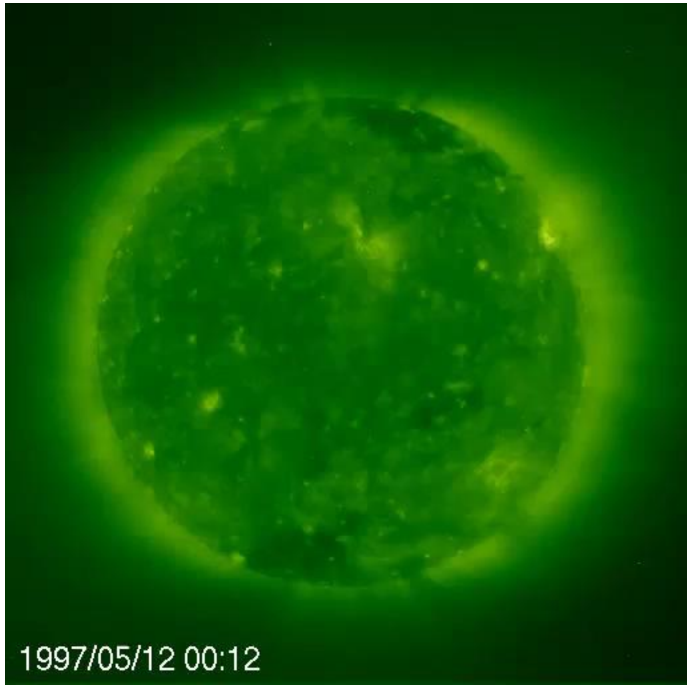

Reconnection results in: Post eruption arcade (flare) and coronal flux rope (magnetic cloud) :

$$\boxed{\Phi_P = \Phi_r}$$

Longcope et al. 2007
Qiu et al. 2007
Gopalswamy et al. 2017

Where does the energy come from?

Extrapolated field lines on TRACE coronal images

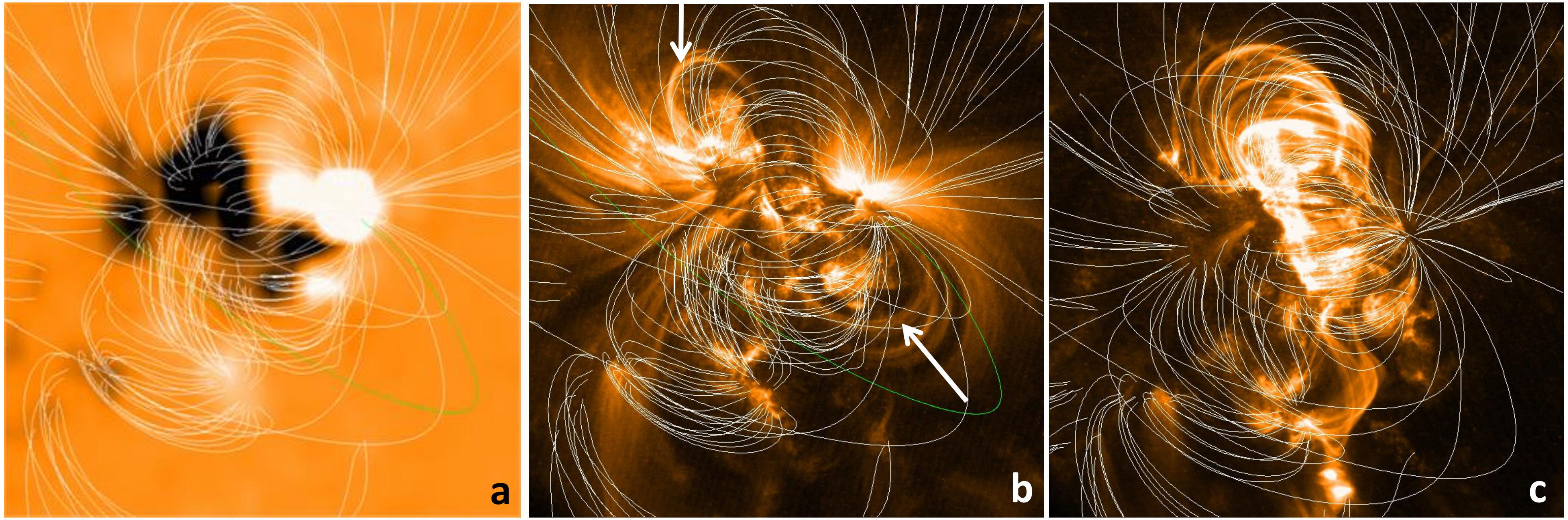

2005/05/13 14:56:00 | 2005/05/13 15:25:56 | 2005/05/13 21:26:36

Photospheric magnetogram with potential field extrapolation

Actual coronal structure is "distorted" from potential field → free energy (FE)
Distortion due to current J.
Lorentz force JxB propels the CME

Free energy went into the CME kinetic energy
Arcade is now potential (no more current J)

De Rosa & Schrijver

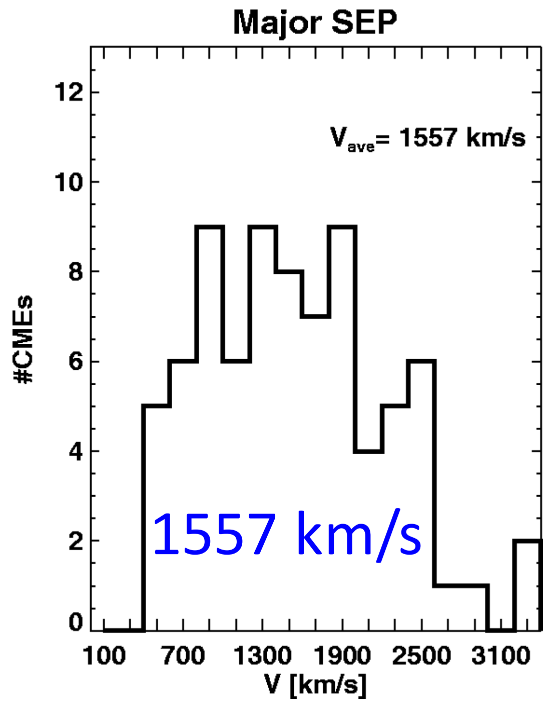

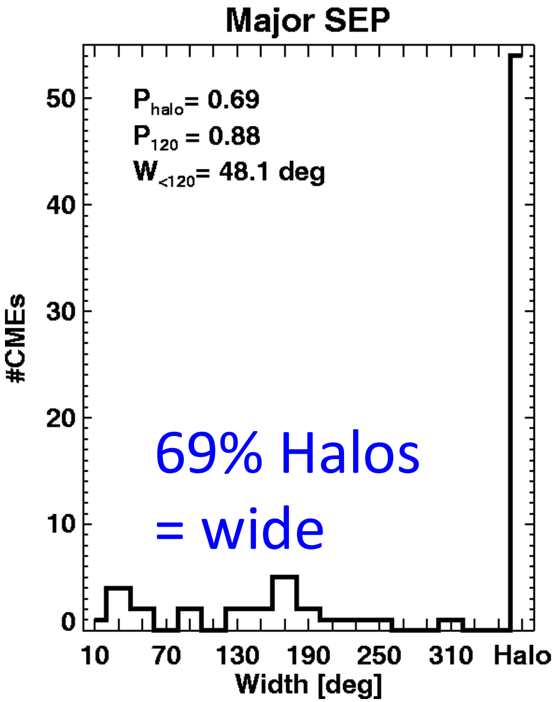

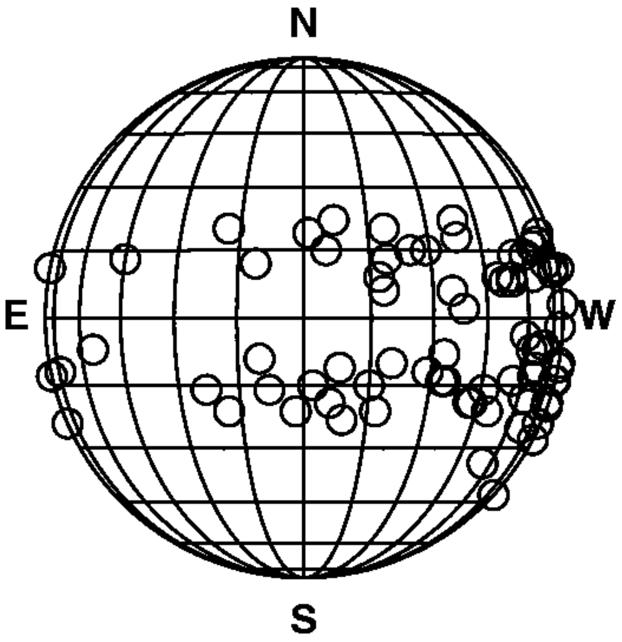

Strong shock
Magnetic connectivity
(Outer structure)

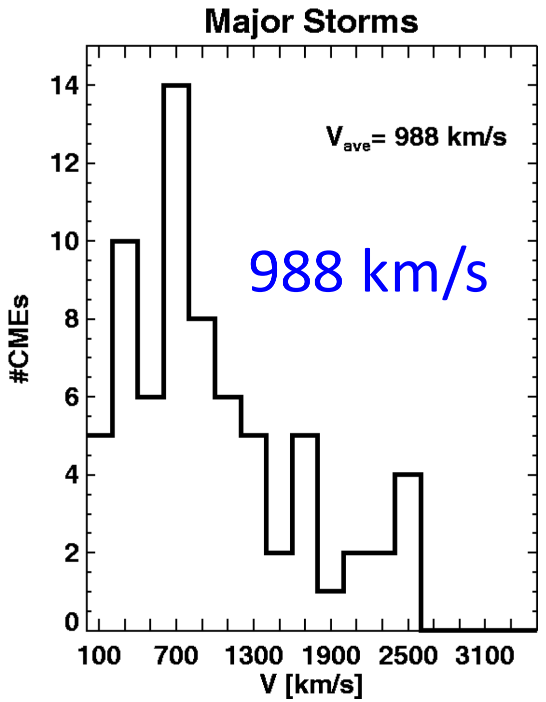

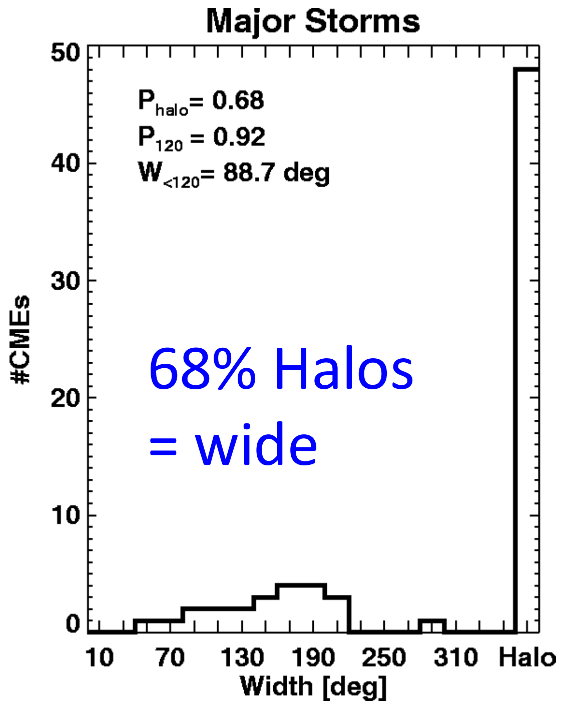

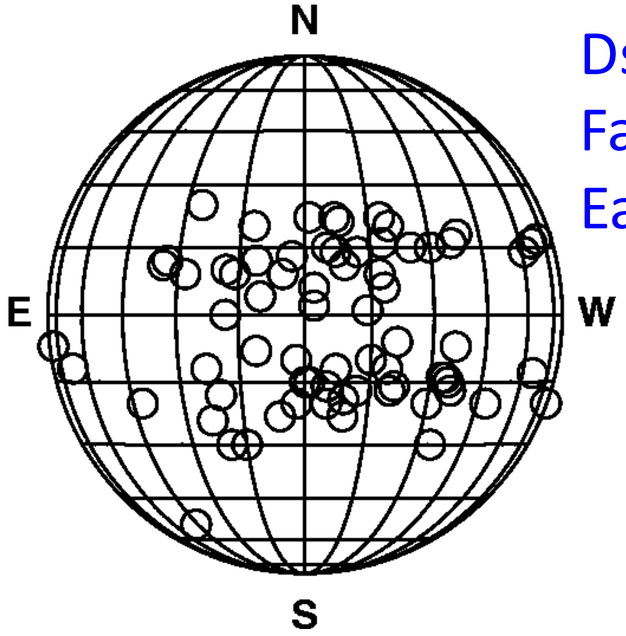

Dst = -0.01VBz – 32 nT
Fast, large –Bz,
Earth-directed CMEs
(Inner Structure)

CME Speed Range

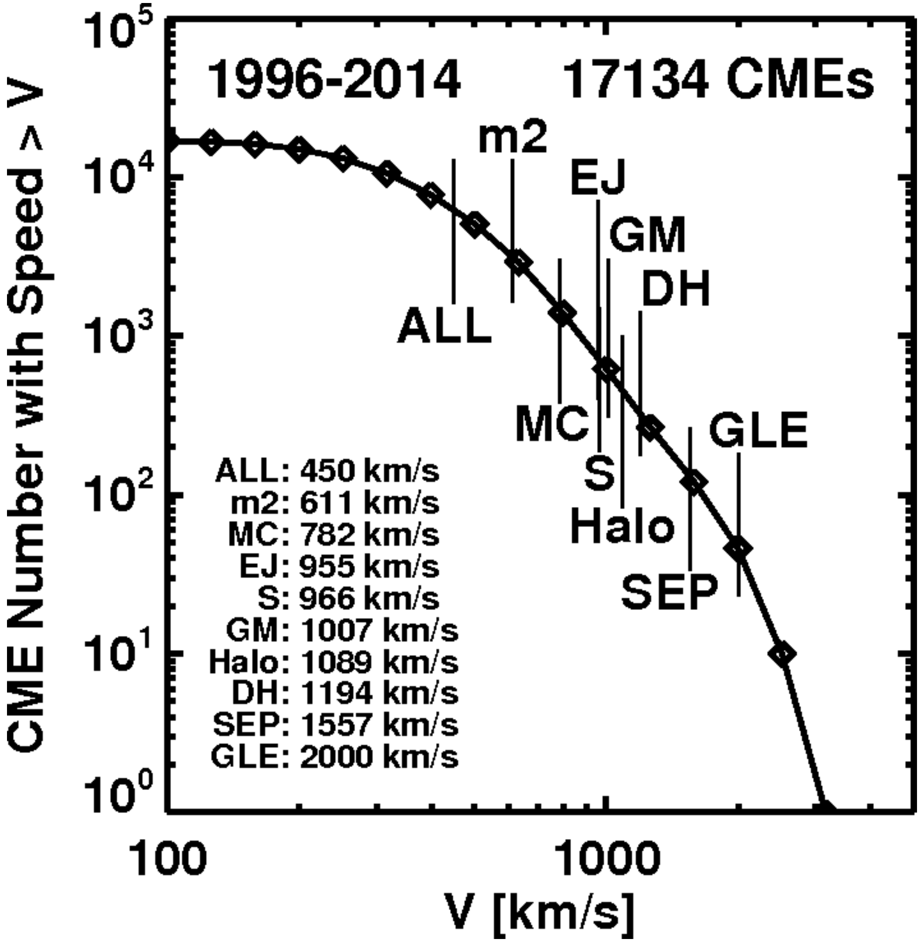

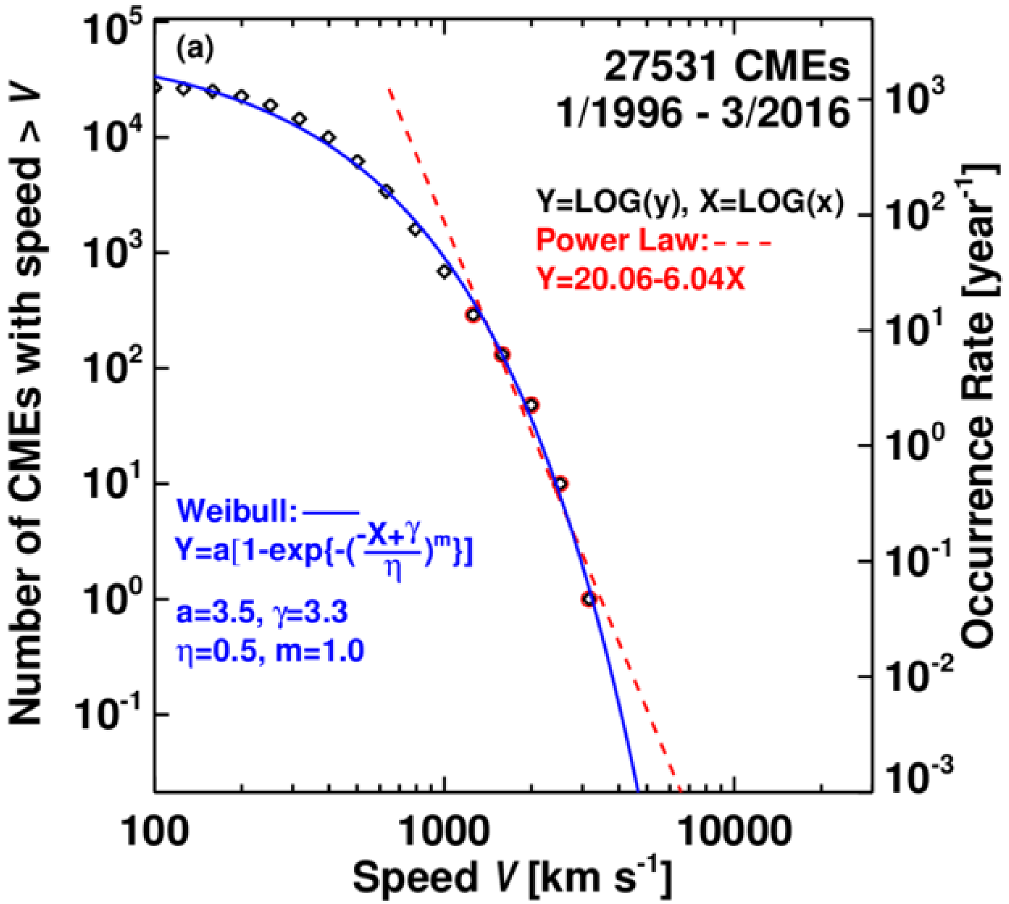

CME speed < ~4000 km/s → Limit to the
Free energy available in active regions (size, B)

100: 3800 km/s
1000: 4700 km/s

CME Speed and Kinetic Energy

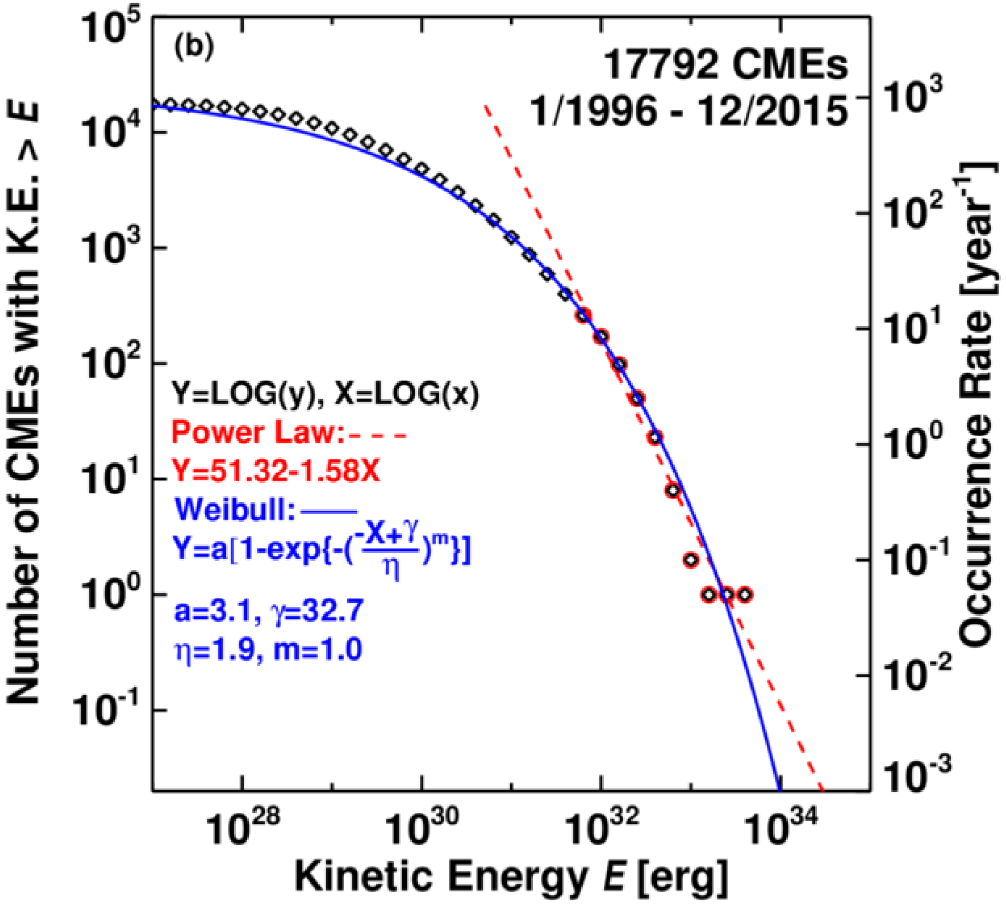

1-in-100 yr: 4.4×10^{33} erg
1-in-1000 yr: 9.8×10^{33} erg

G et al. 2018

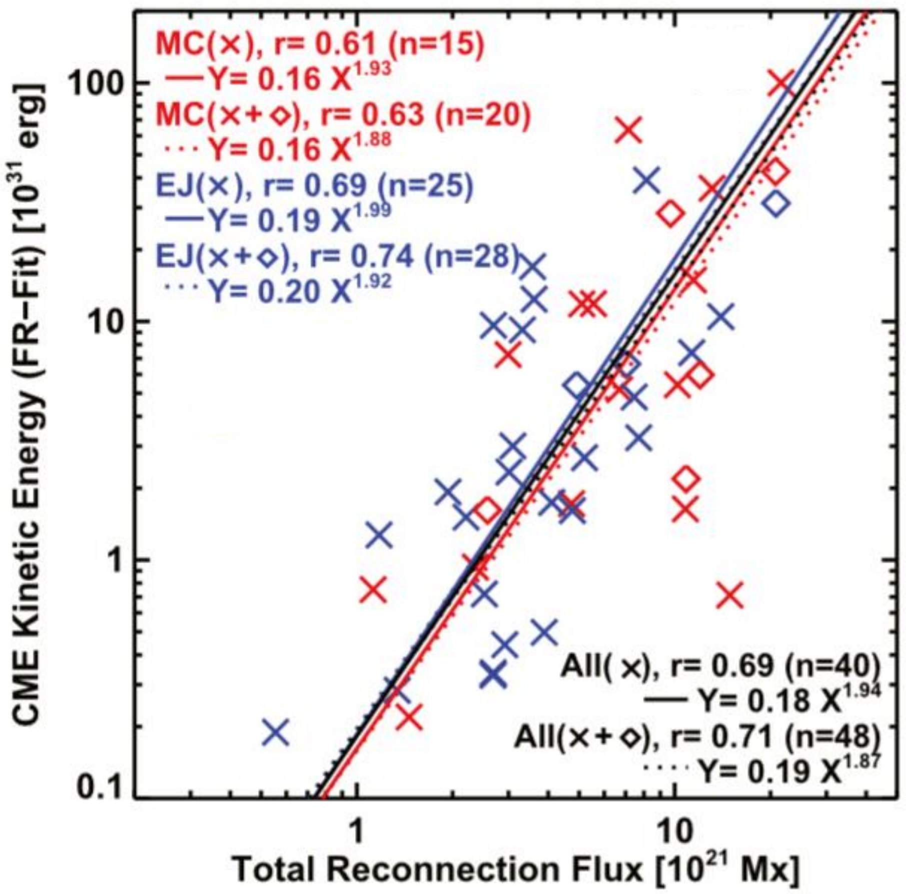

- B = 6100 G (Livingston+ 2006), A = 6000 msh (Newton 1955).
- AR flux Φ_{AR} ~1.12×10^{24} Mx.

If 10% of AR flux becomes reconnected in an eruption, a 1000-year CME is possible

CME Rate & Speed (Rotation Averaged)

- The CME rate is slightly higher in cycle 23
- The average speed is lower
- The number of energetic CMEs is lower in cycle 24

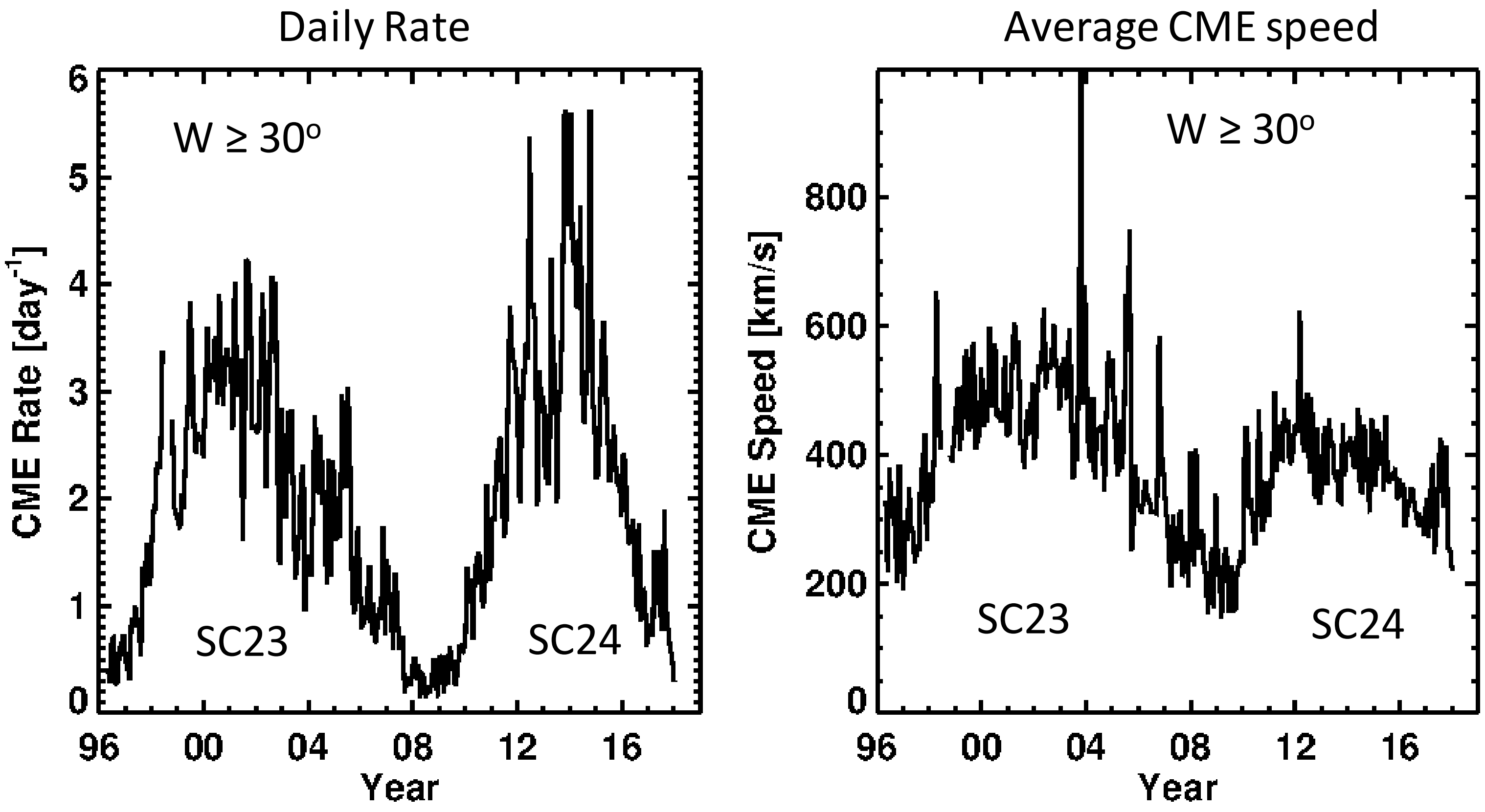

The rate is ~0.5 per day during the solar minimum and exceed ~3.5 per day during solar maximum

The CME speed also varies with solar cycle: CMEs are generally faster during solar maxima

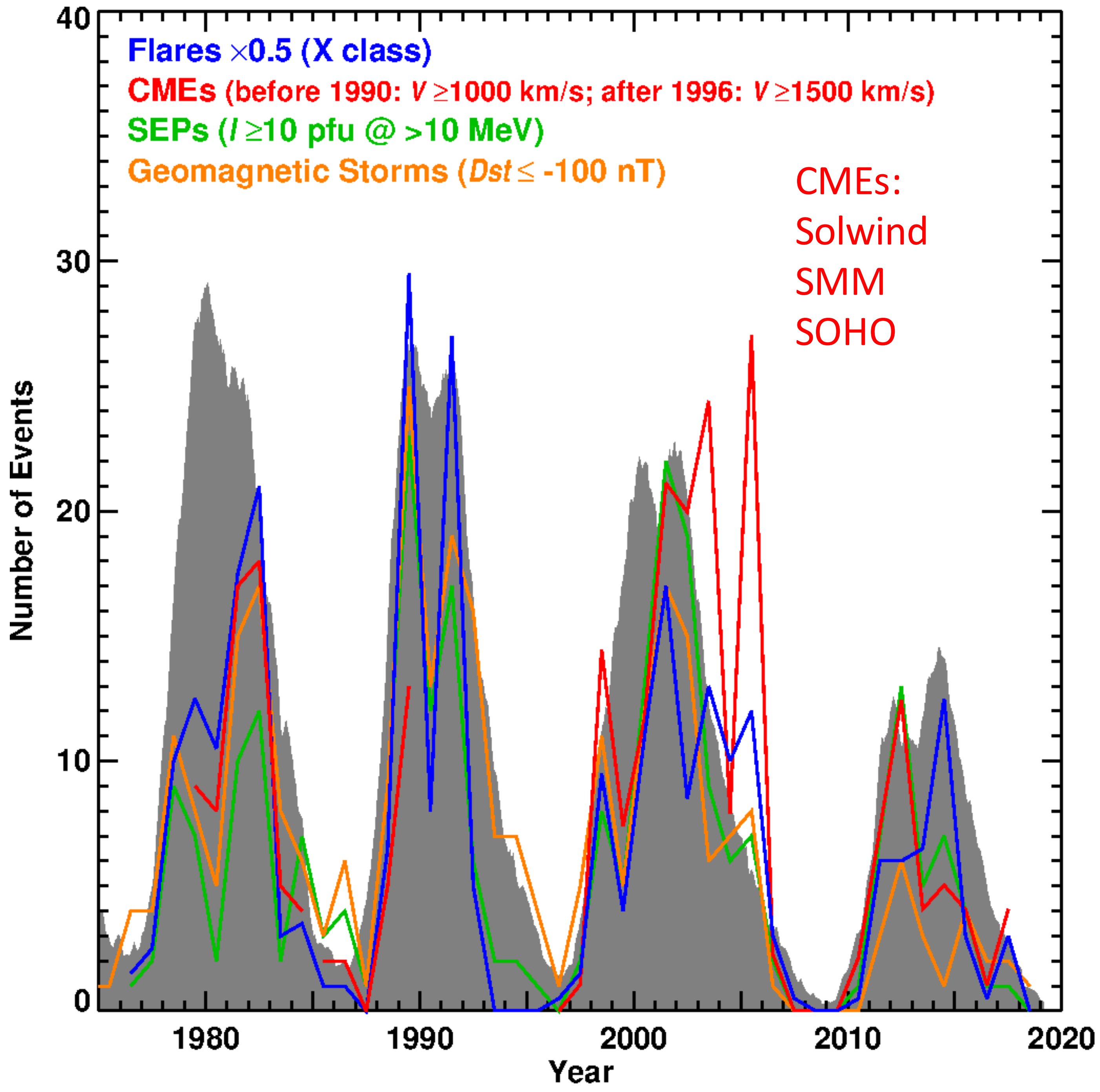

Flares, CMEs, SEPs & Magnetic Storms

- General correlation, but many exceptions: e.g. more flares in the second SSN peak in SC 24, but less SWx events
- Flares can be observed from anywhere on the disk
- About 10% of X-class flares are non-eruptive
- SEPs and magnetic storms from non-spot regions: non-spot CMEs

Great Magnetic Storms from Large Spots

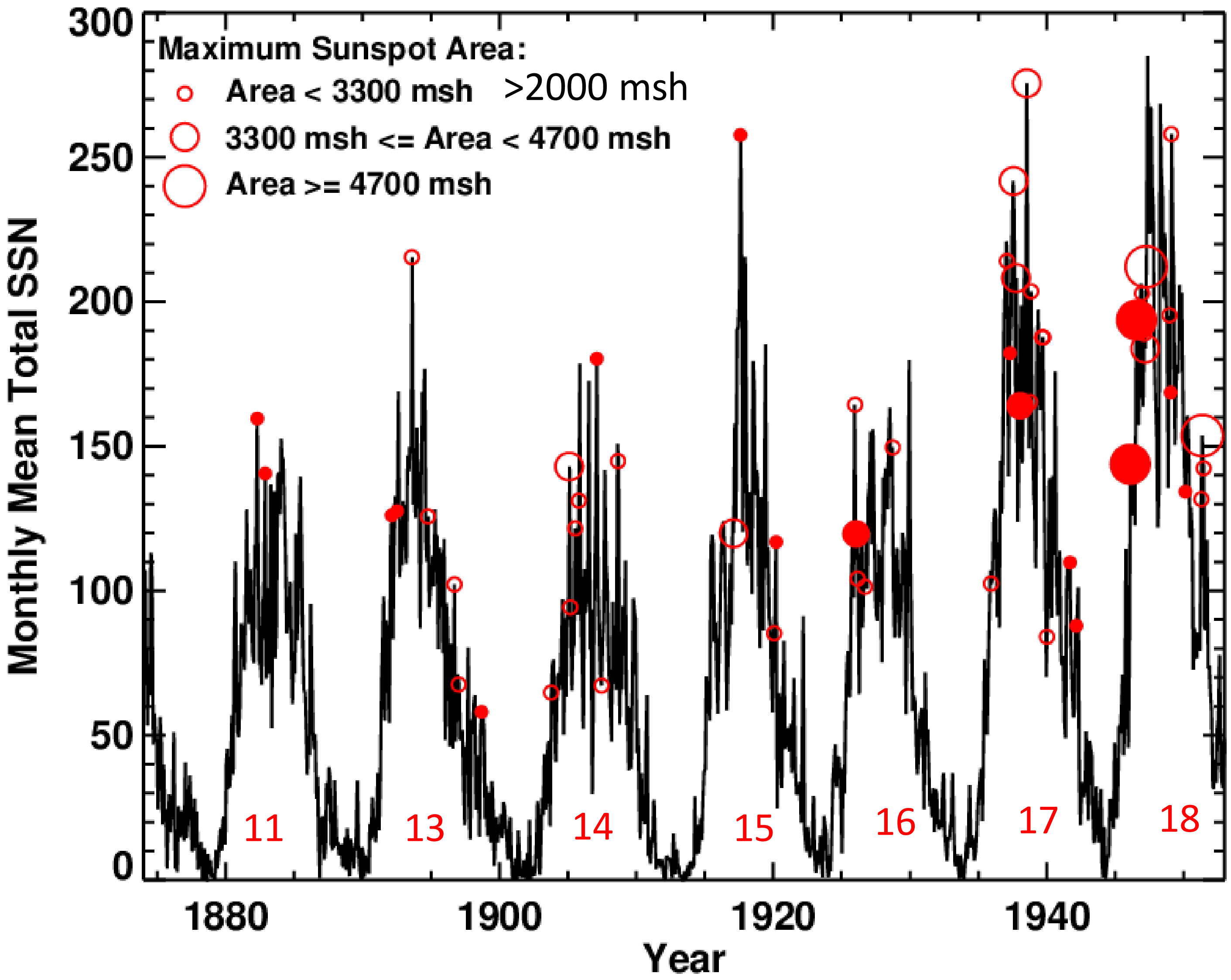

SSN: SILSO
SS Area & Great Storms: Newton 1955

2013/09/29 Filament Eruption

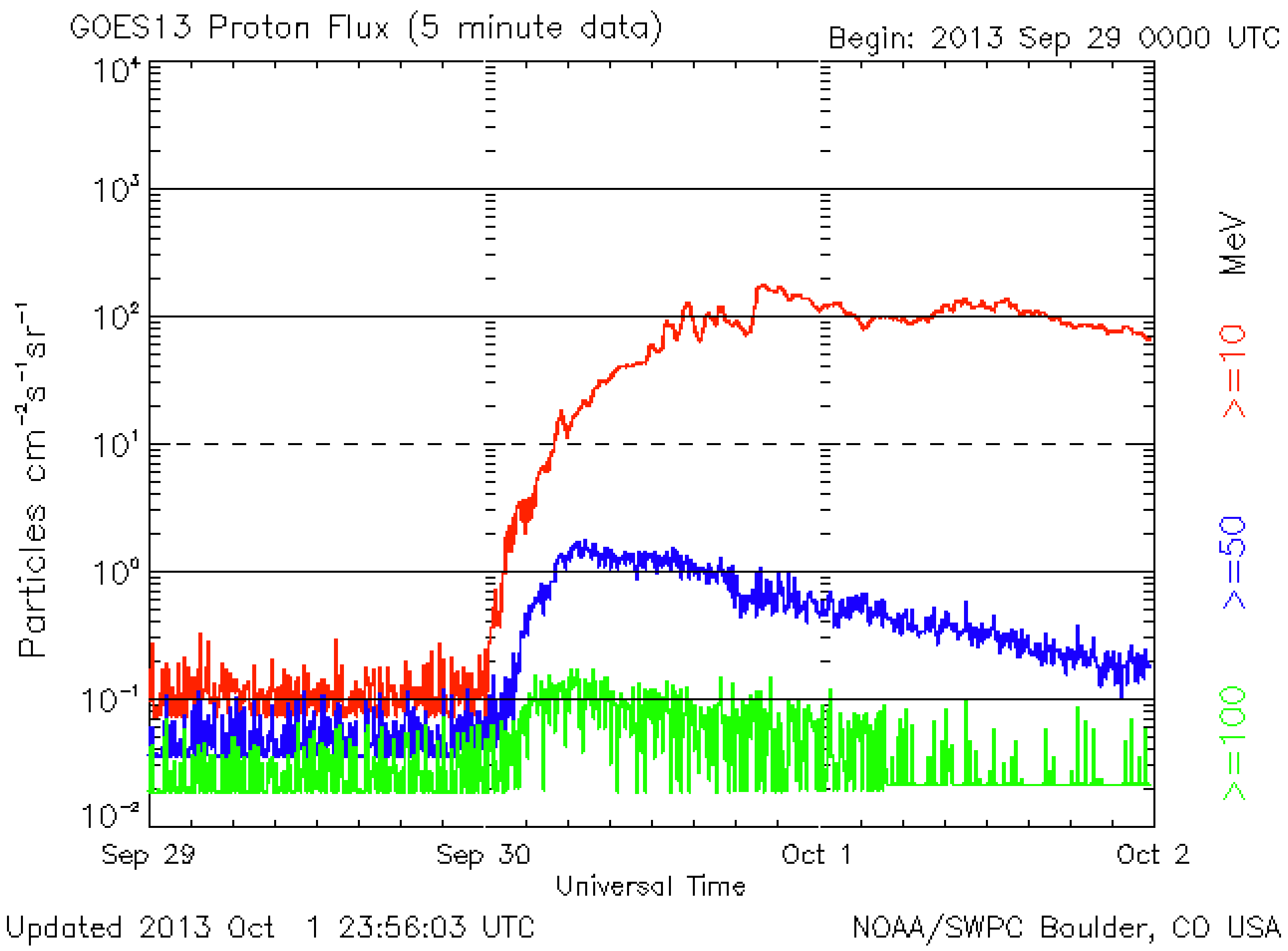

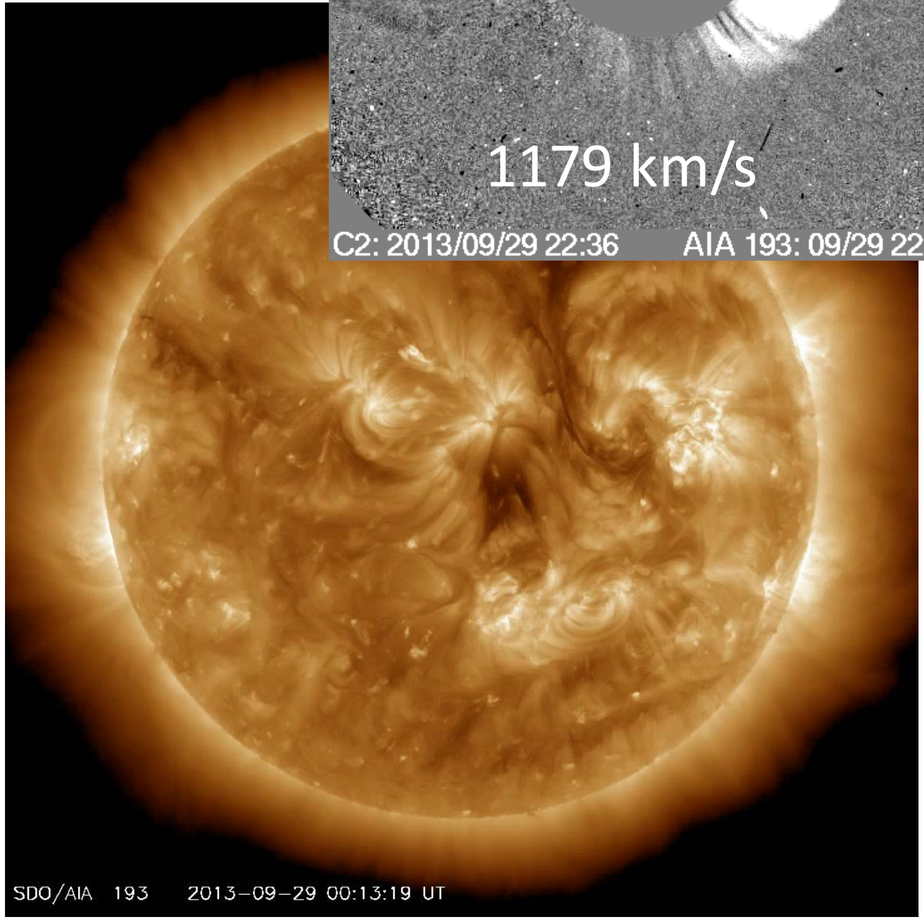

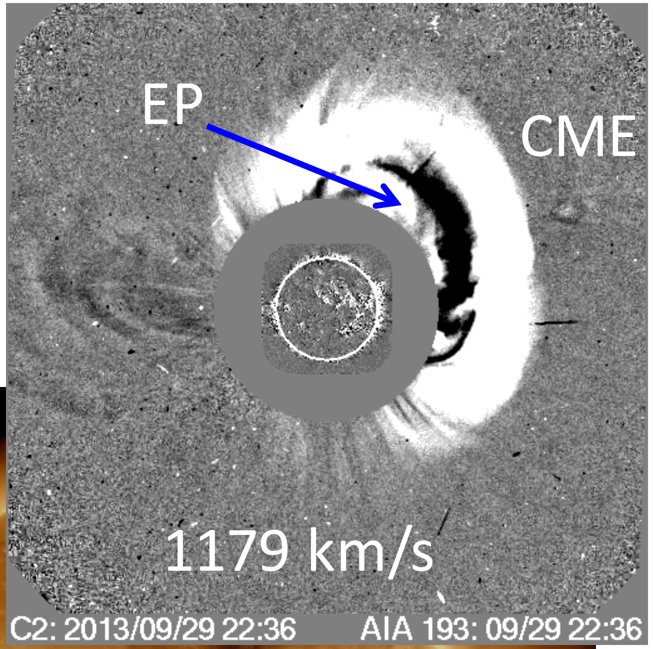

G et al. 2015 ApJ

SSN – CME Rate

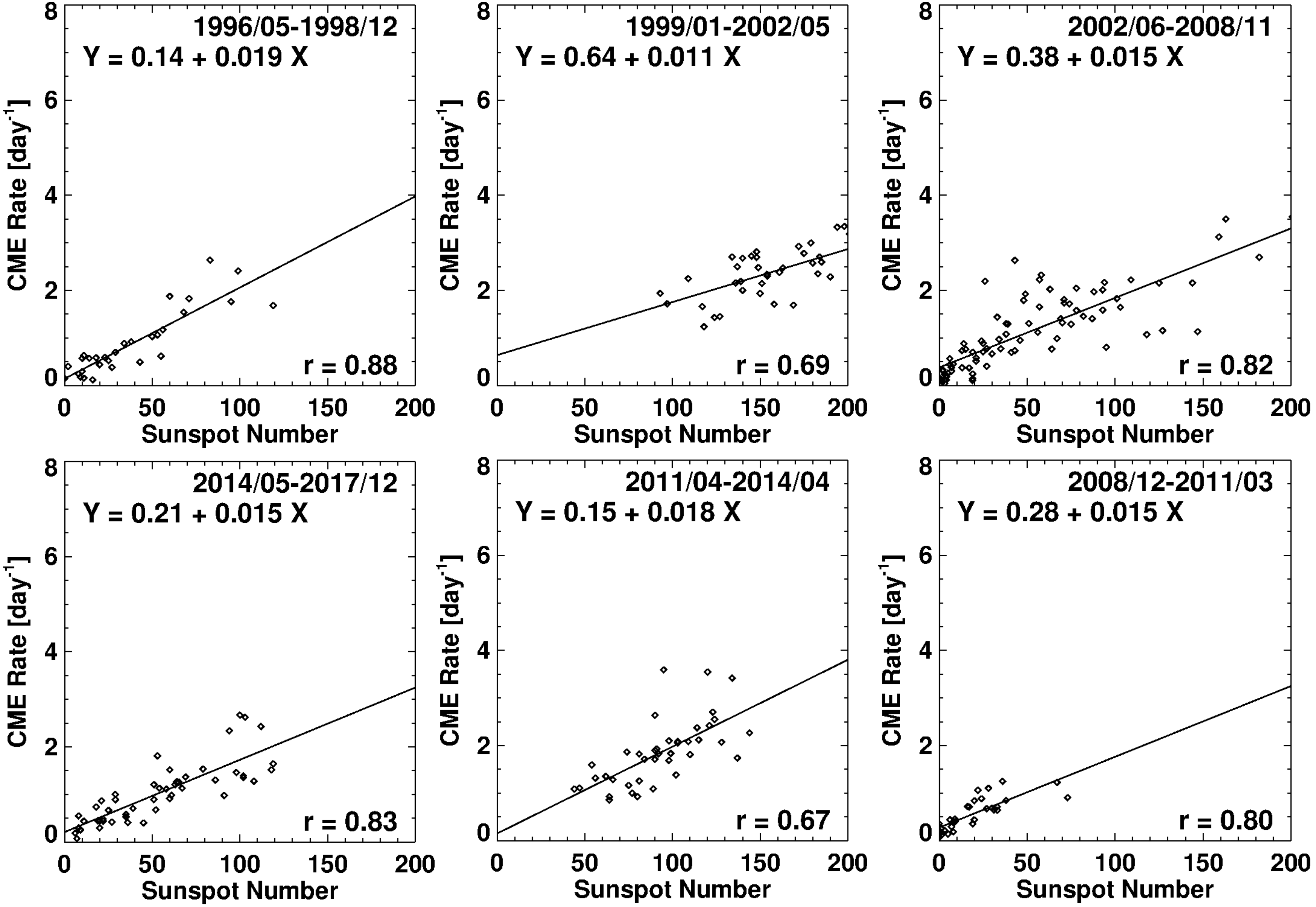

Correlations are similar in corresponding phases

Max phases have weaker CME-SSN correlation

Rise phases are similar in SC 23 & 24

Max & decl phases are different in SSN

CMEs from non-spot magnetic regions

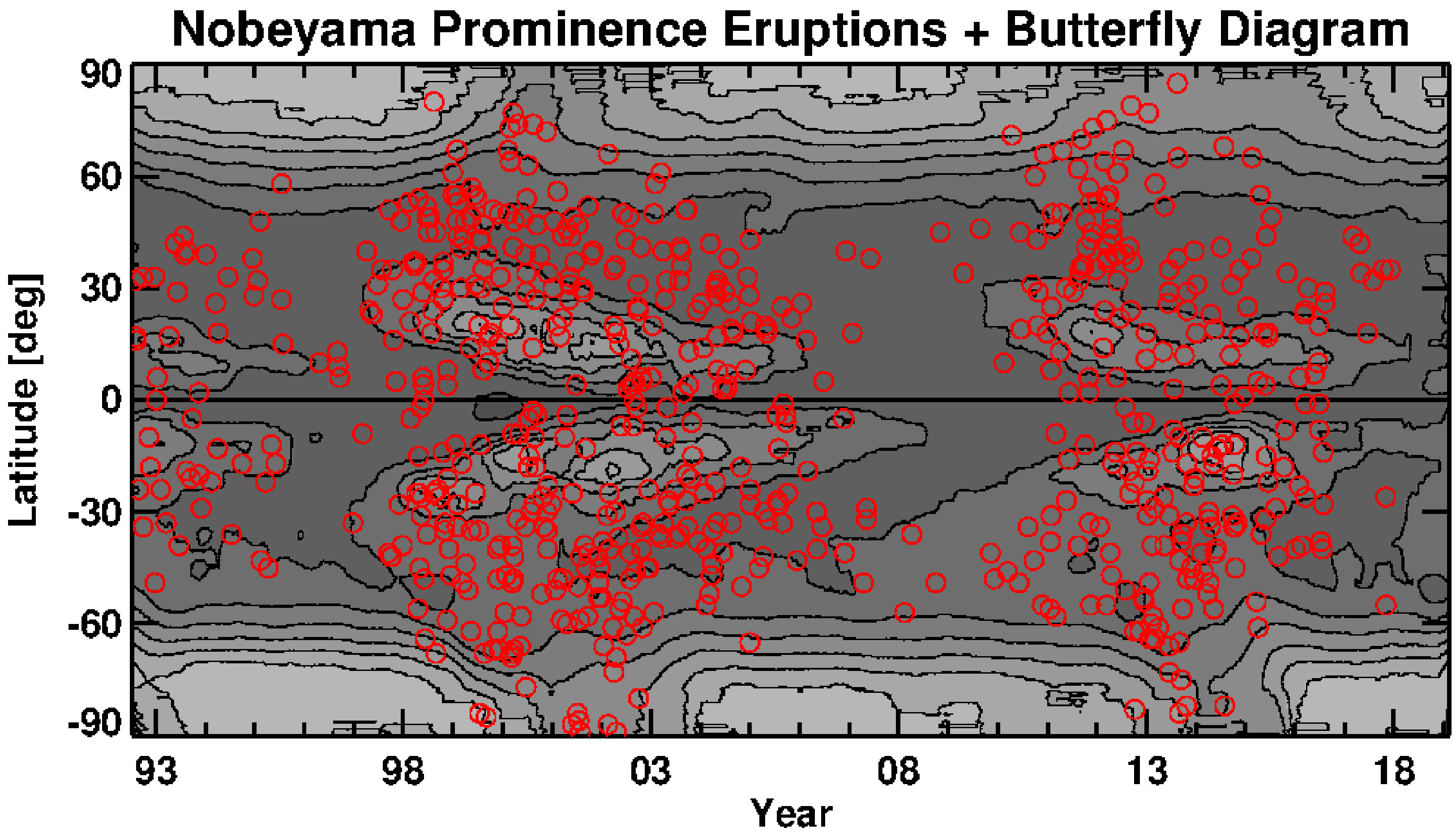

Locations of prominence eruptions (PEs) automatically detected from Nobeyama Radioheliograph images

Many CMEs from mid and high latitude magnetic regions (filament regions outside active regions)

CMEs and Geomagnetic Storms

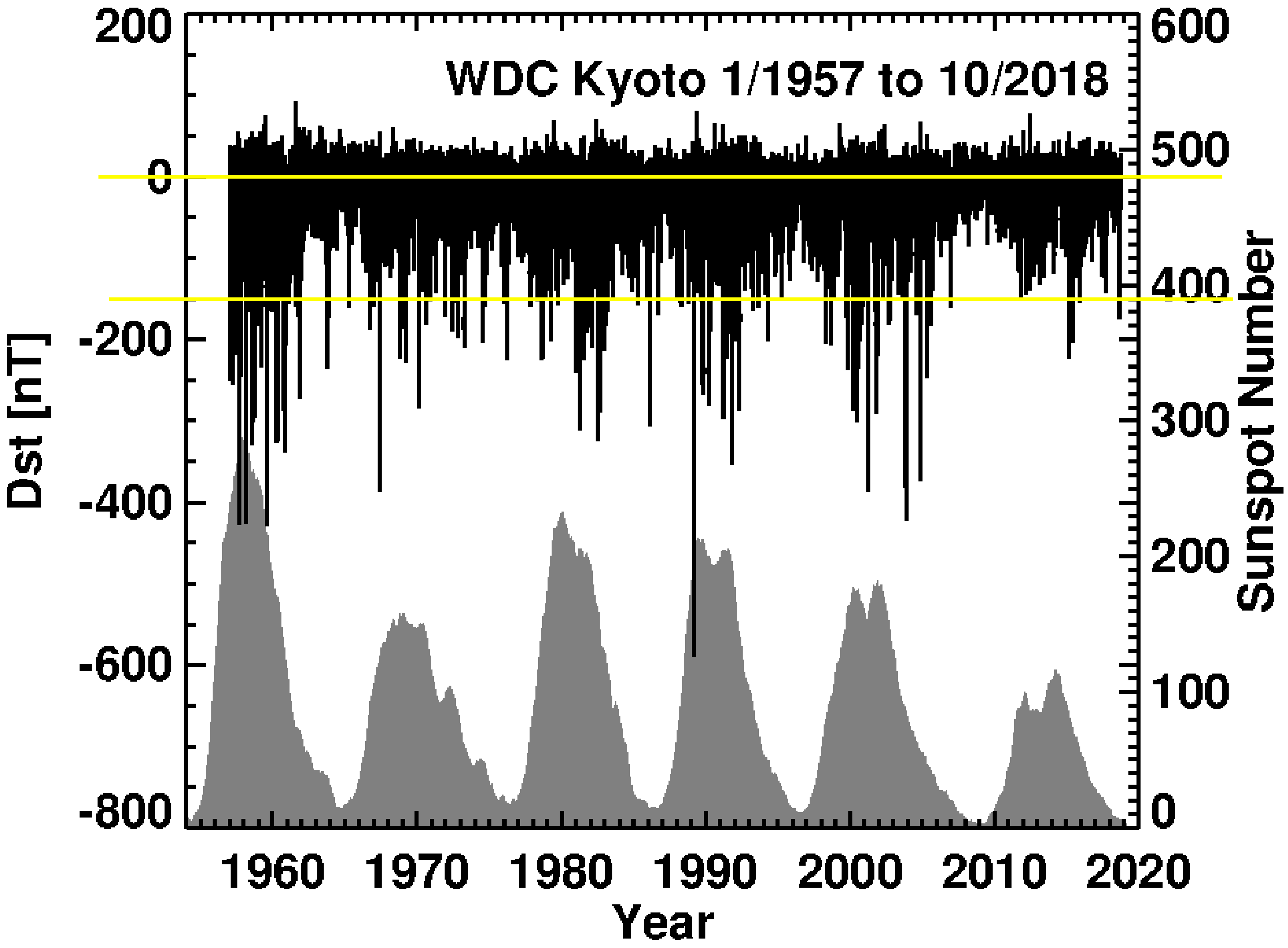

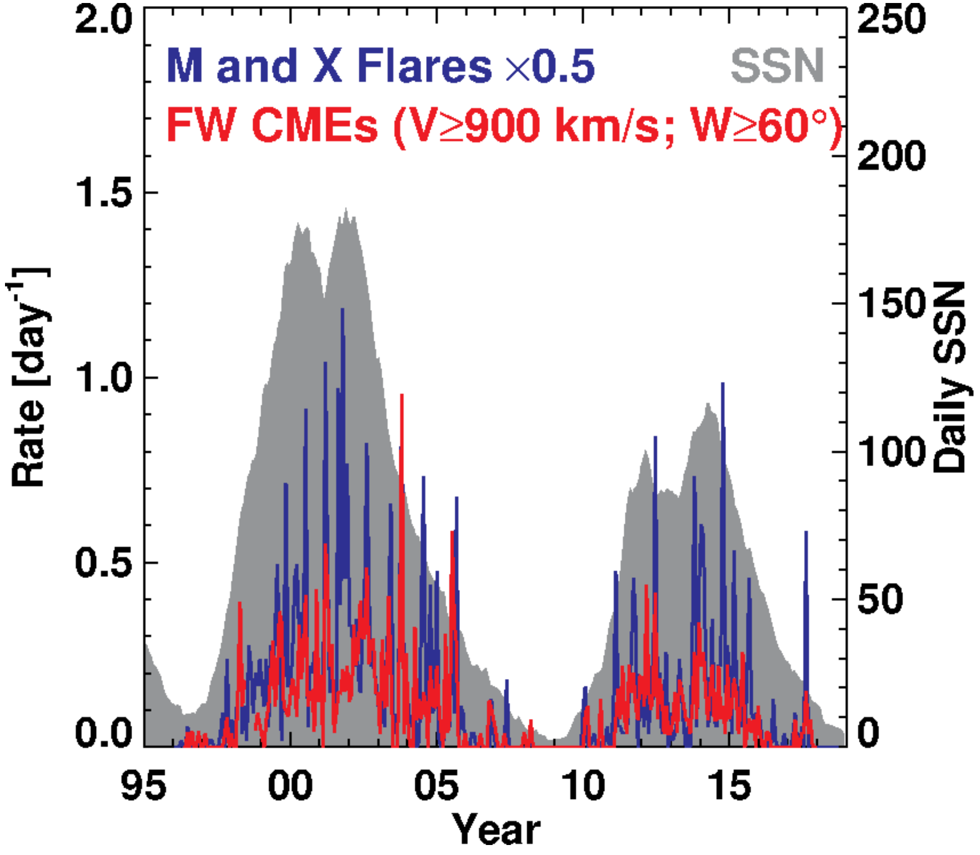

Strange Behavior in Cycle 24

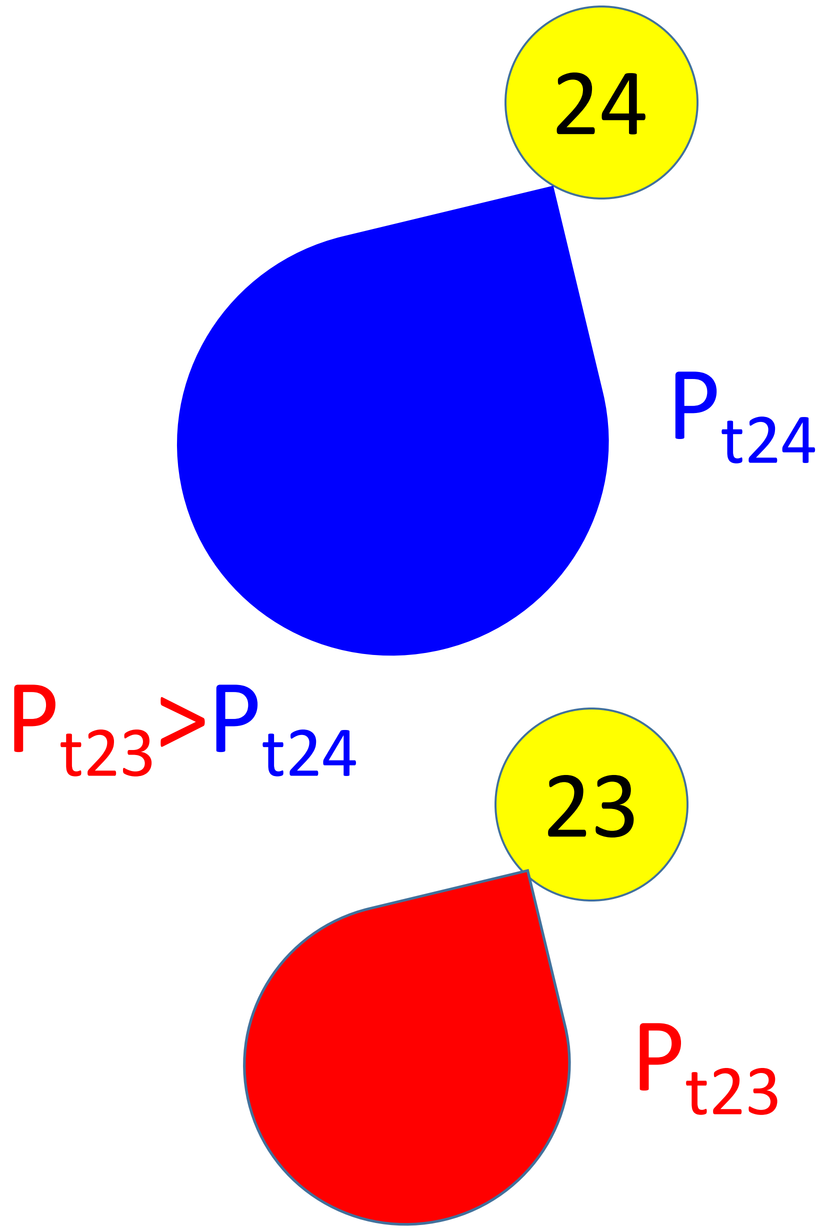

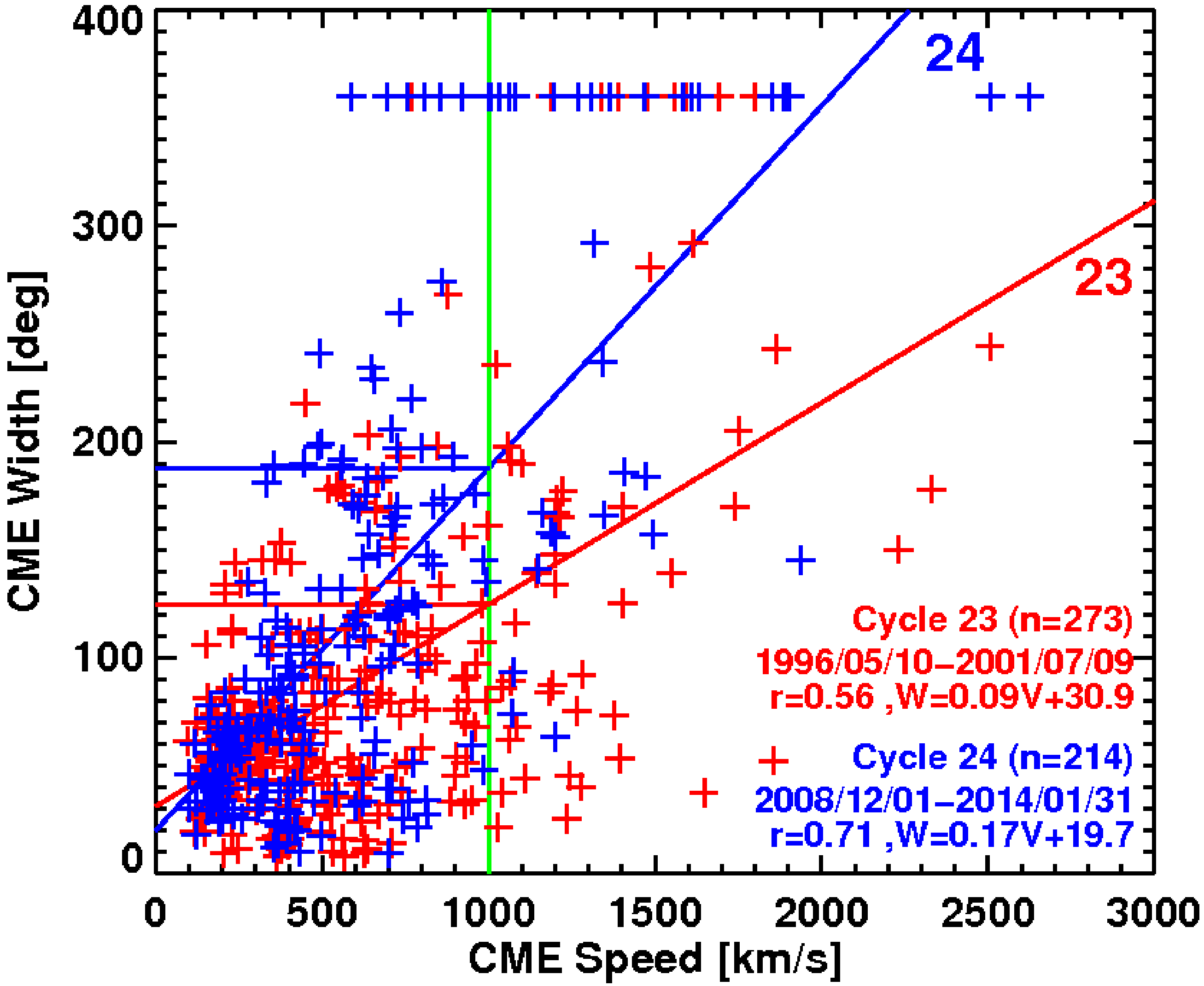

Regions with different CME productivity (Sep 2017)

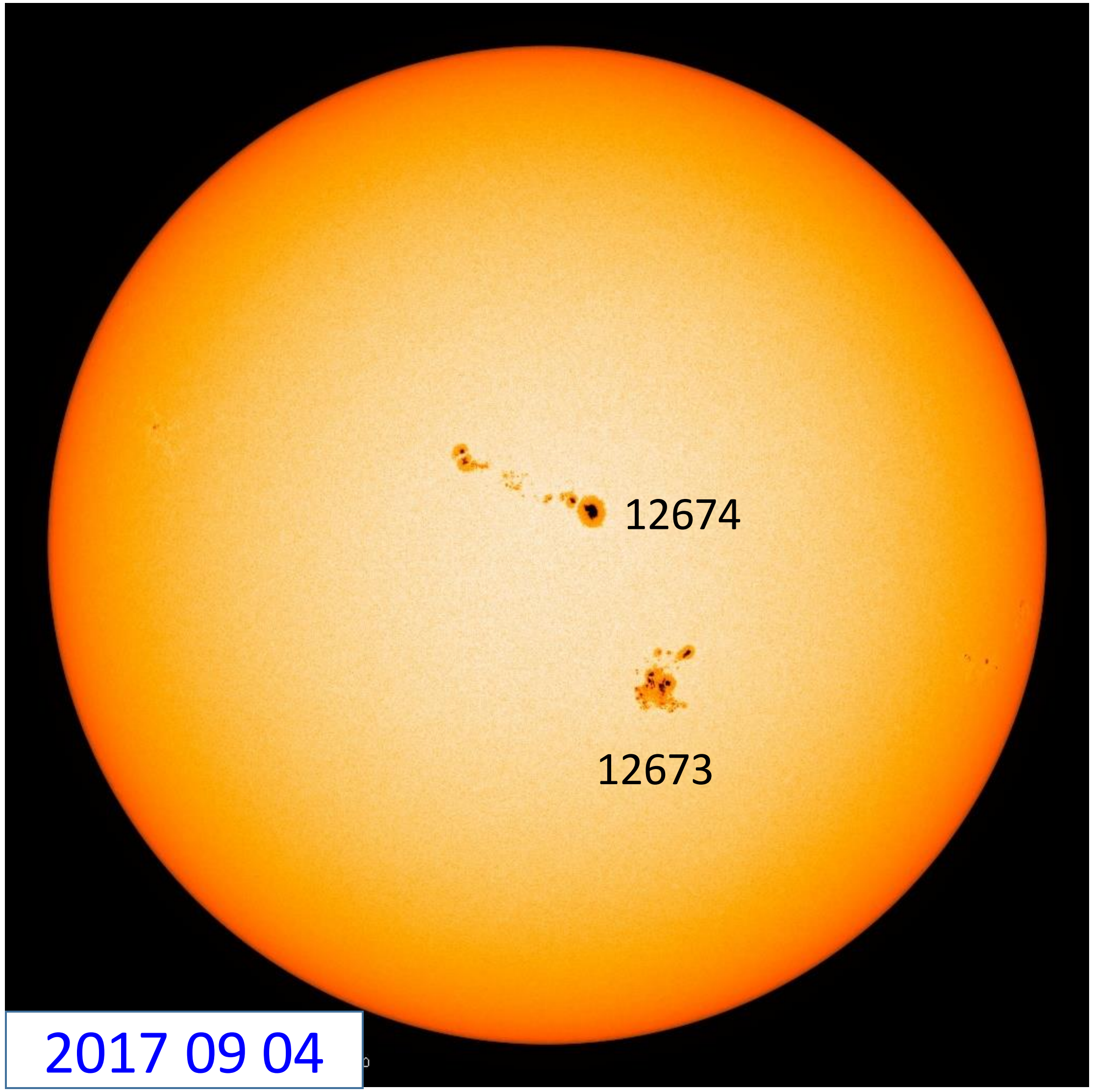

SDO/AIA Continuum

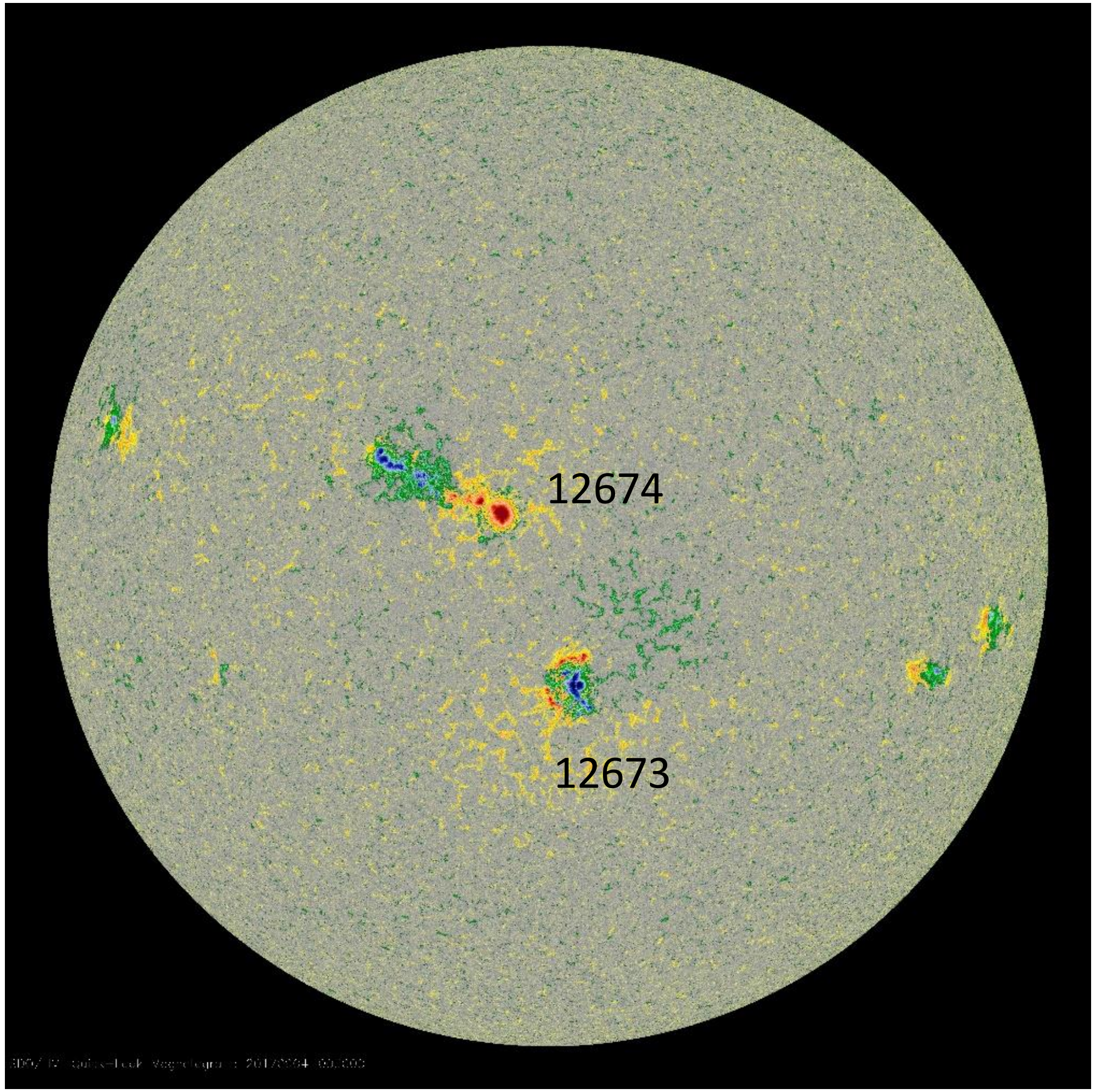

SDO/HMI Magnetogram

Flares & CMEs in ARs 12673 & 12674

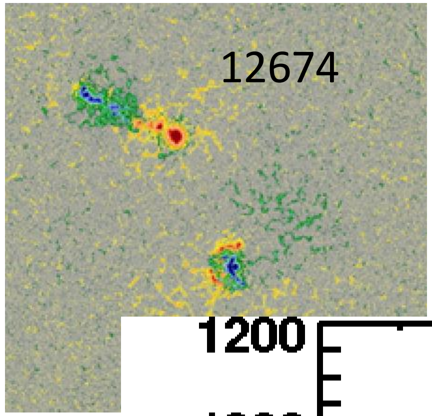

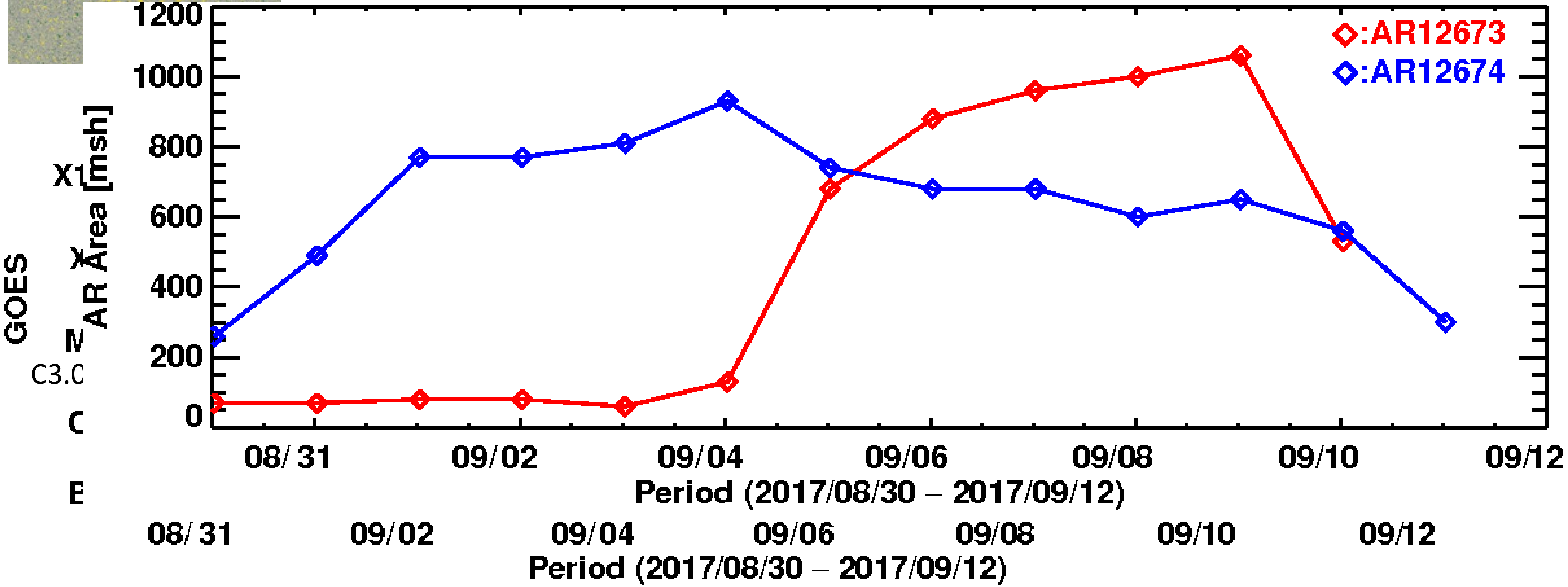

Space weather events occurred from AR 12673 when the region rotated from the disc center to the west limb. The Sep 06 CME caused both a major mag storm & a large SEP event. The Sep 4 CME had a large SEP event and minor storm; Sep 10 CME had a GLE; Sep 6 & 10 CMEs had sustained gamma-ray emission

High Latitude CMEs

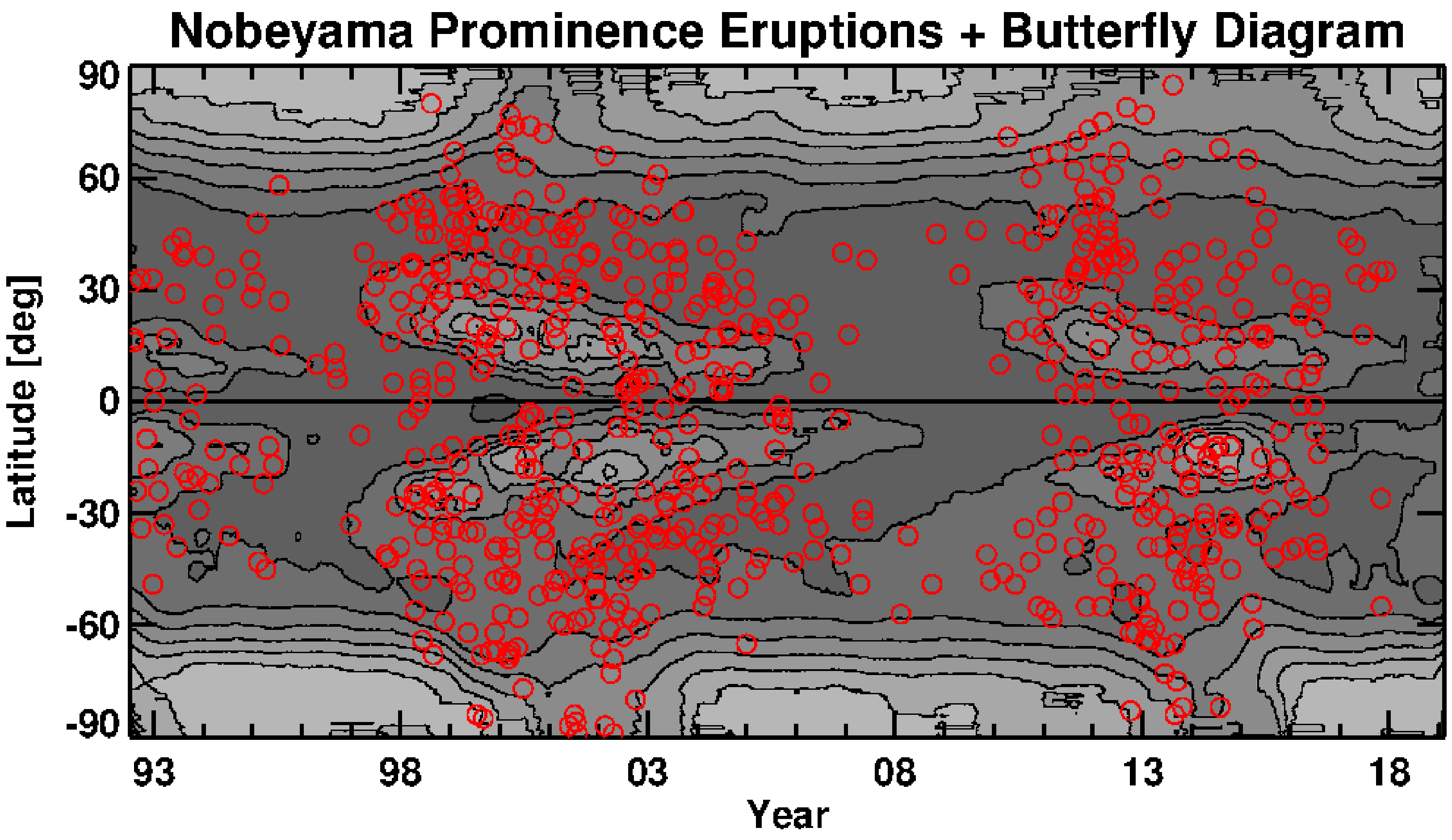

Locations of prominence eruptions (PEs) automatically detected from Nobeyama Radioheliograph images

Battle Between Incumbent and Insurgent Fluxes

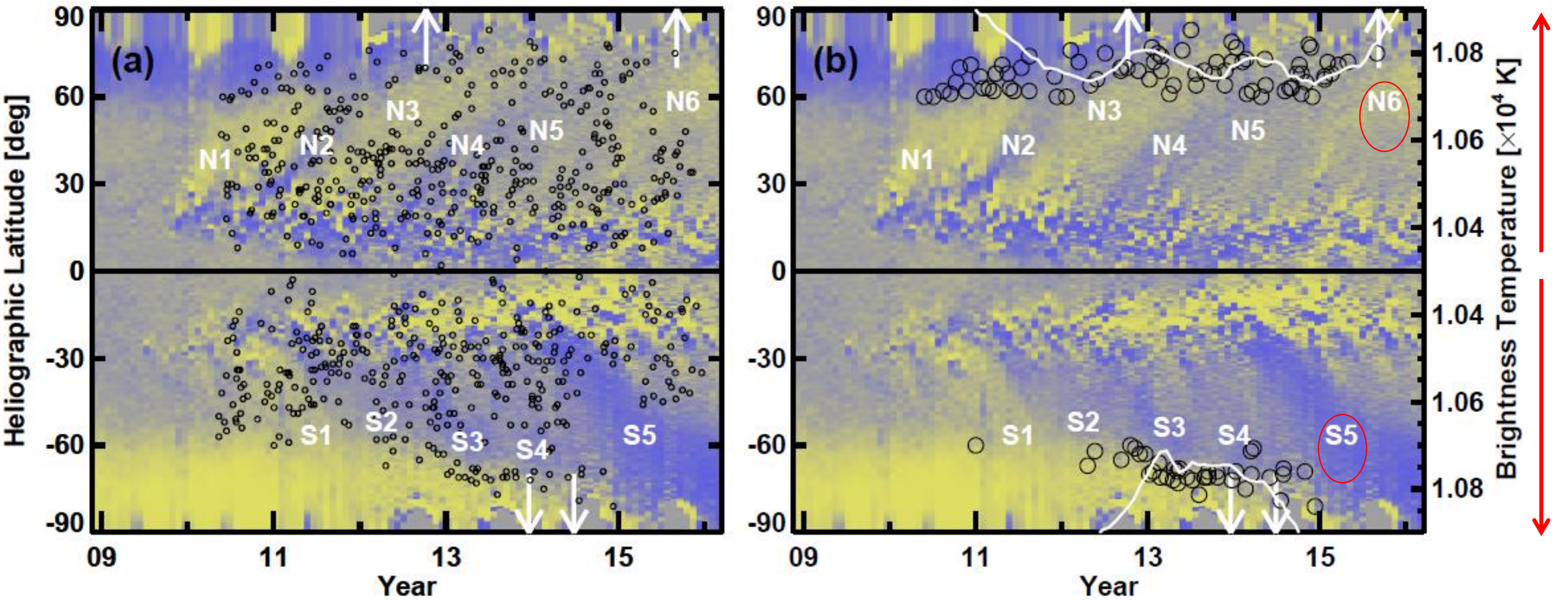

- After reversal, no bipolar regions – No eruptions -- polar Tb increases above quiet Sun level (new polarity B)
- Delayed reversal: the surges of "wrong polarity" N2, N4, N5 (Cameron+ 2013; Jiang et al. 2014; Sun et al. 2015)
- After sign reversal → increase in HL Tb indicating buildup of new polarity field

Reversal asymmetry: SN (expected: NS - Svalgaard & Kamide 2013)

G et al. 2016 ApJL

Kodaikanal, India K-line Prominence areas; HL prominences mark Max phase

Ananthakrishnan 1952 Nature

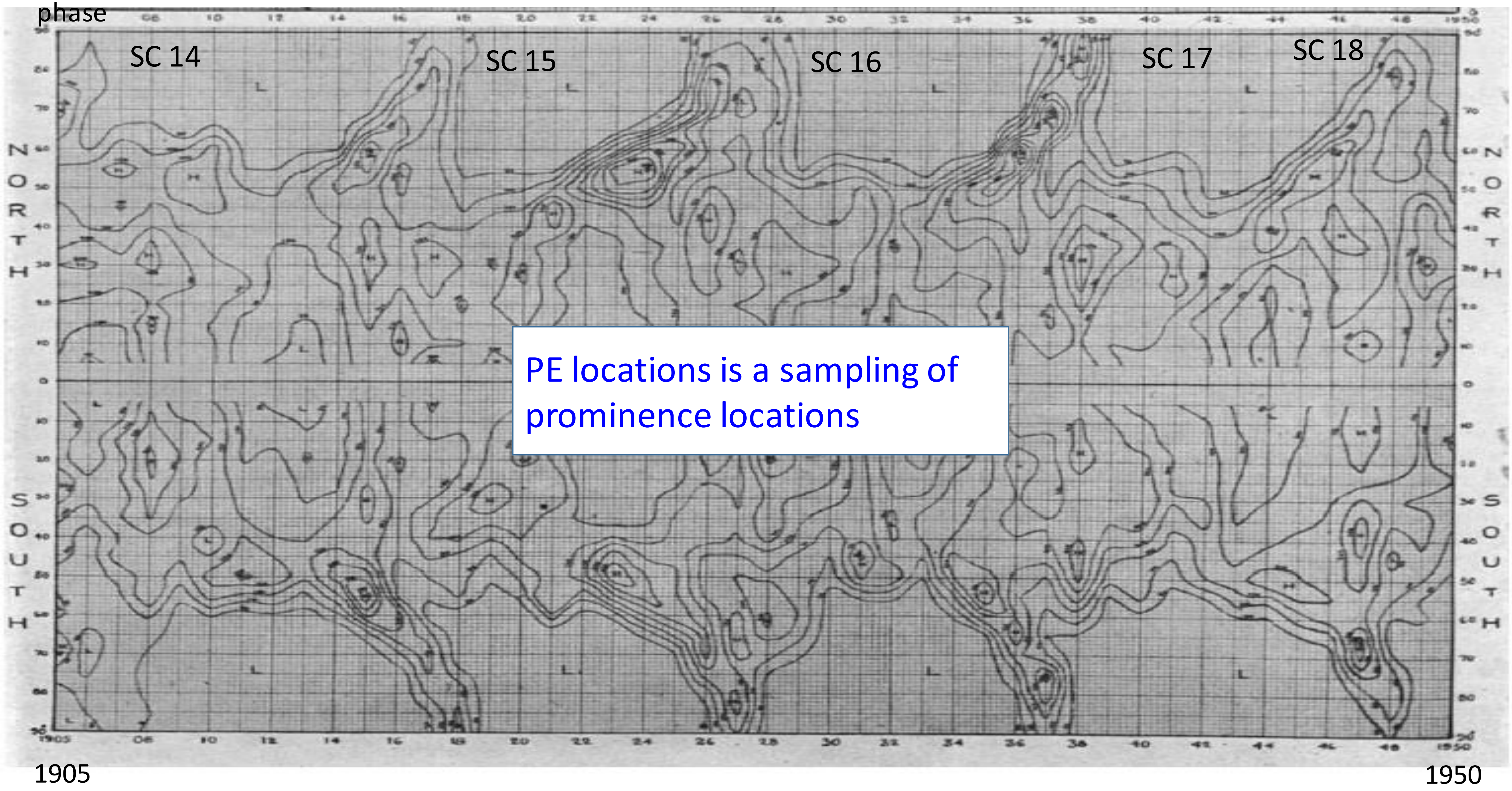

Rush to the Poles of Filaments & Polarity Reversal

1971 April 29
1971.0

1981 Jan 21
1981.0

1990 Dec 11
1991

2000.9

2nd RTTP in SC 20
Otherwise
Reversal
asymmetry would
have been NS
(Waldmeier 1973)

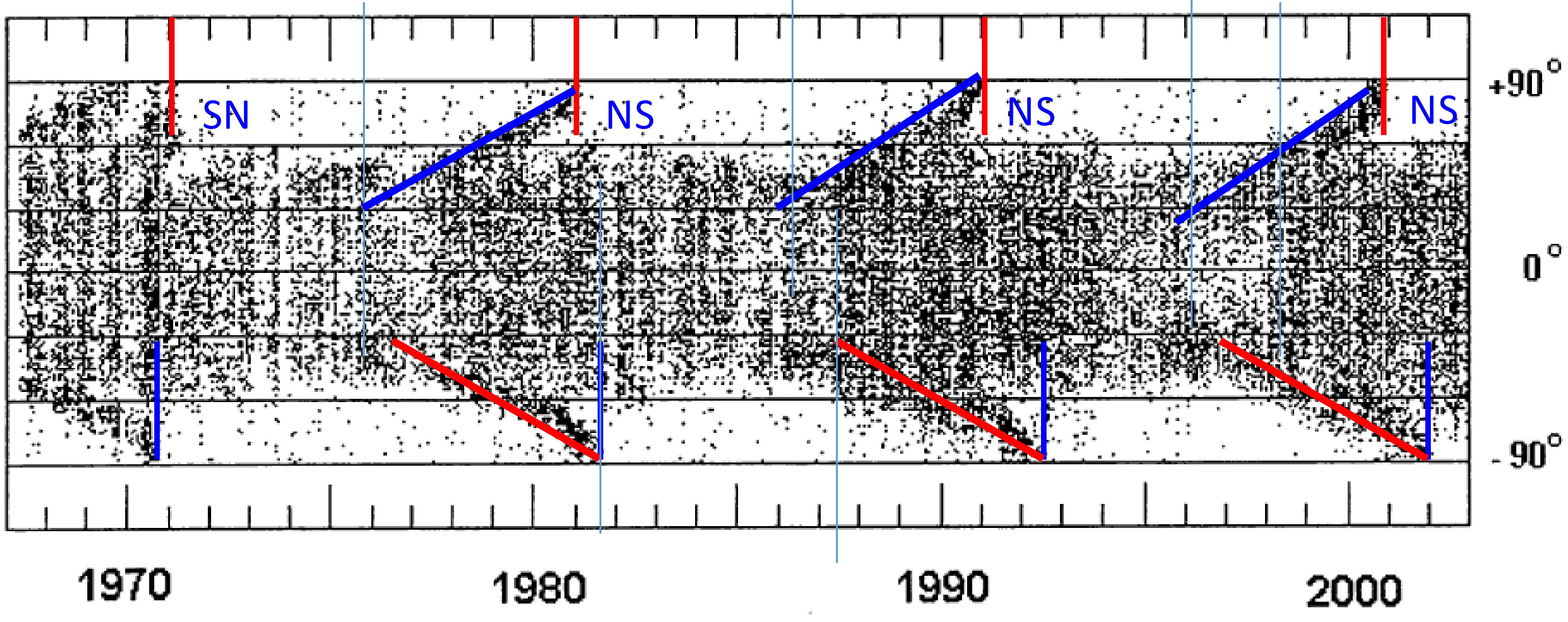

1970.5
1970 Nov

1981.5
1981 Jul10

1992.5
1992 Feb 28

2002

Waldmeier 1960
Hyder 1965
Sync. RTTP &
Sign reversal

SC 20

Lorenc et al. 2003

Historical RTTPs

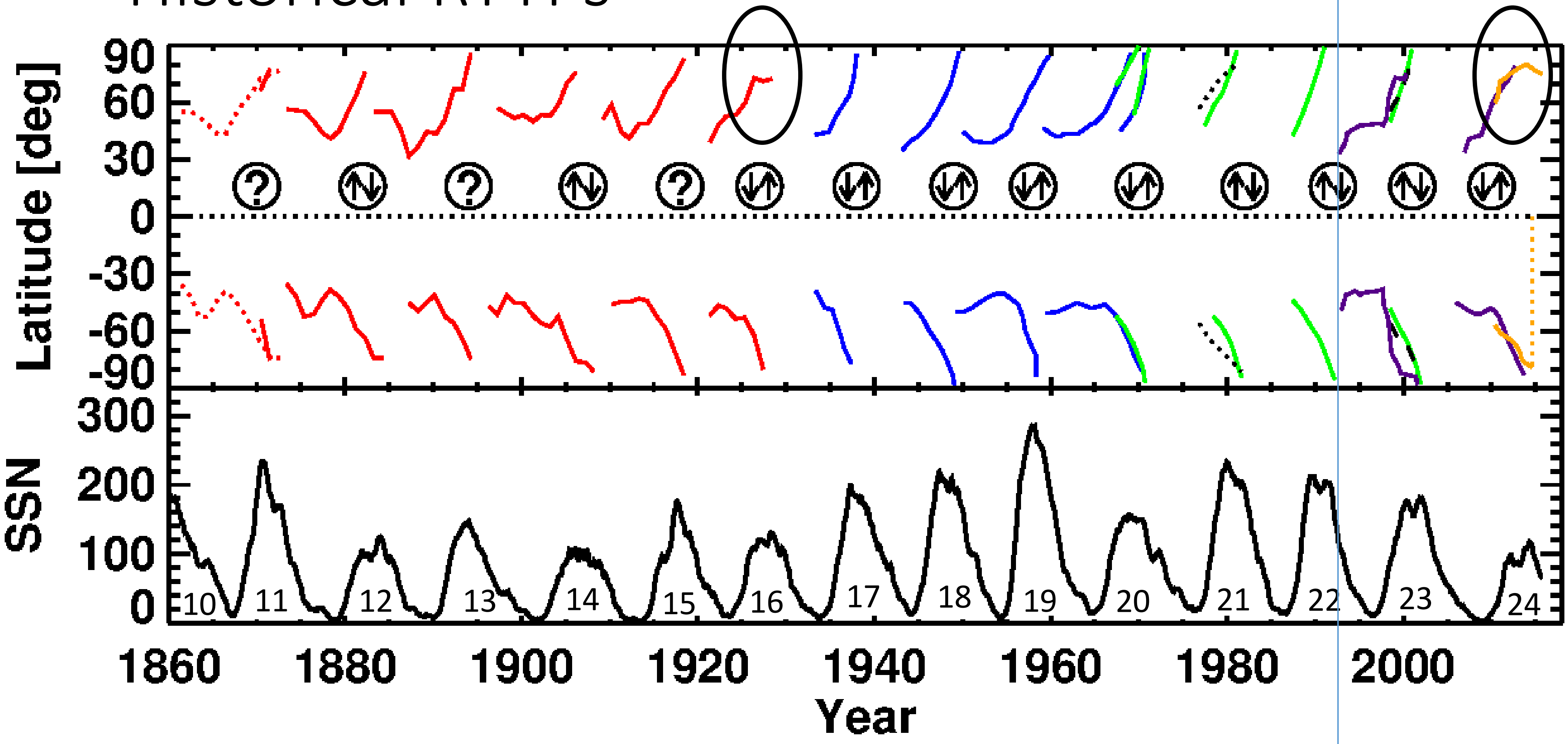

Magenta: PE from NoRH
Orange: PE from SDO
…… Fujimori 1984
------ Pojoga & Huang 2003

10-20: Stix (compiled from Lockyer 1931; Kiepenhauer 1953; Waldmier 1968; 1973)
20-23: Lorenc et al. (2003)
23-24 Gopalswamy et al. 2003; 2012; 2016

G et al. 2018 JASTP

Cycle 16 has similar RTTP behavior as cycle 24; the reversal asymmetry also changes

Kodaikanal, India K-line Prominences

Daily Prom areas - Ananthakrishnan 1952 Nature

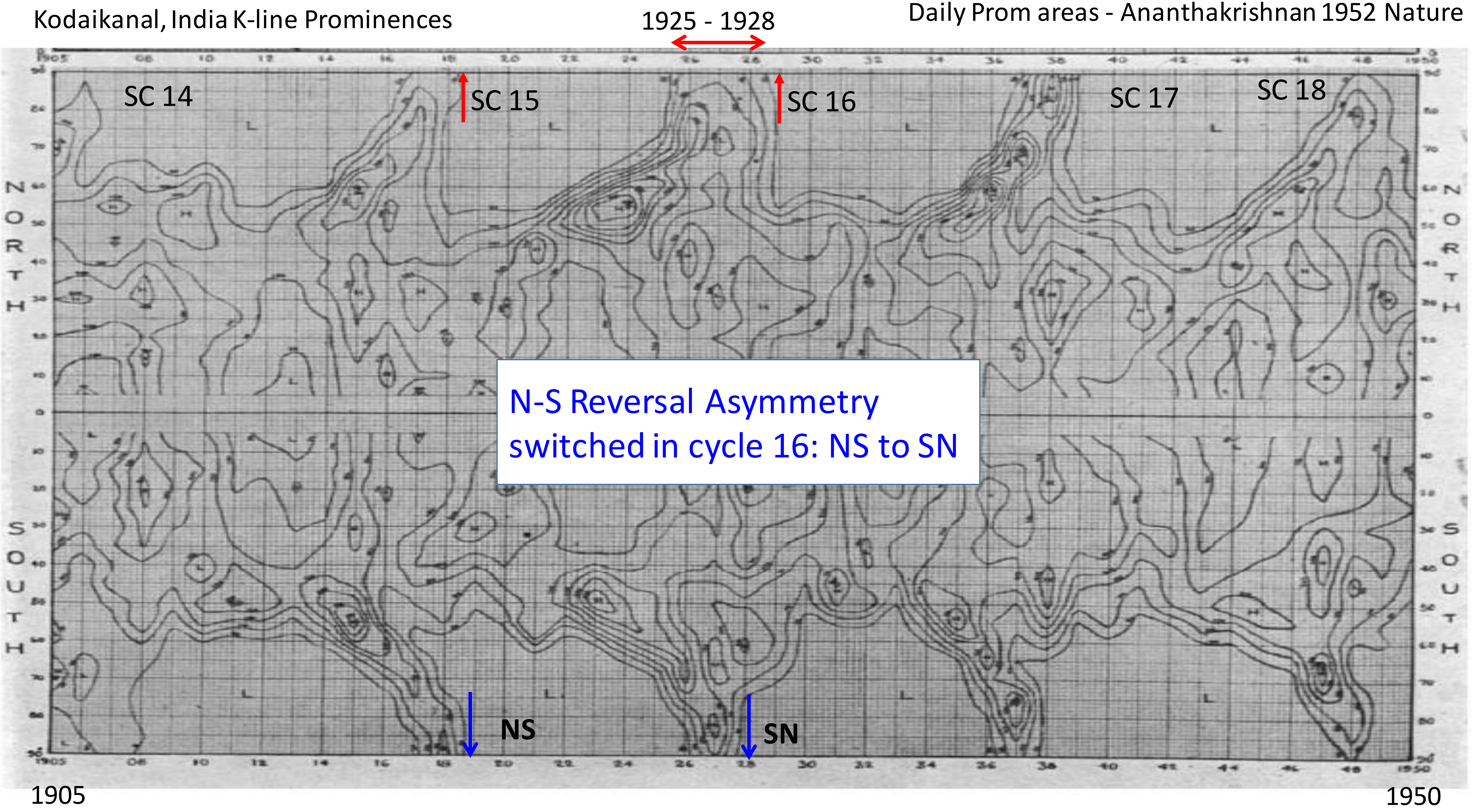

Historical RTTPs

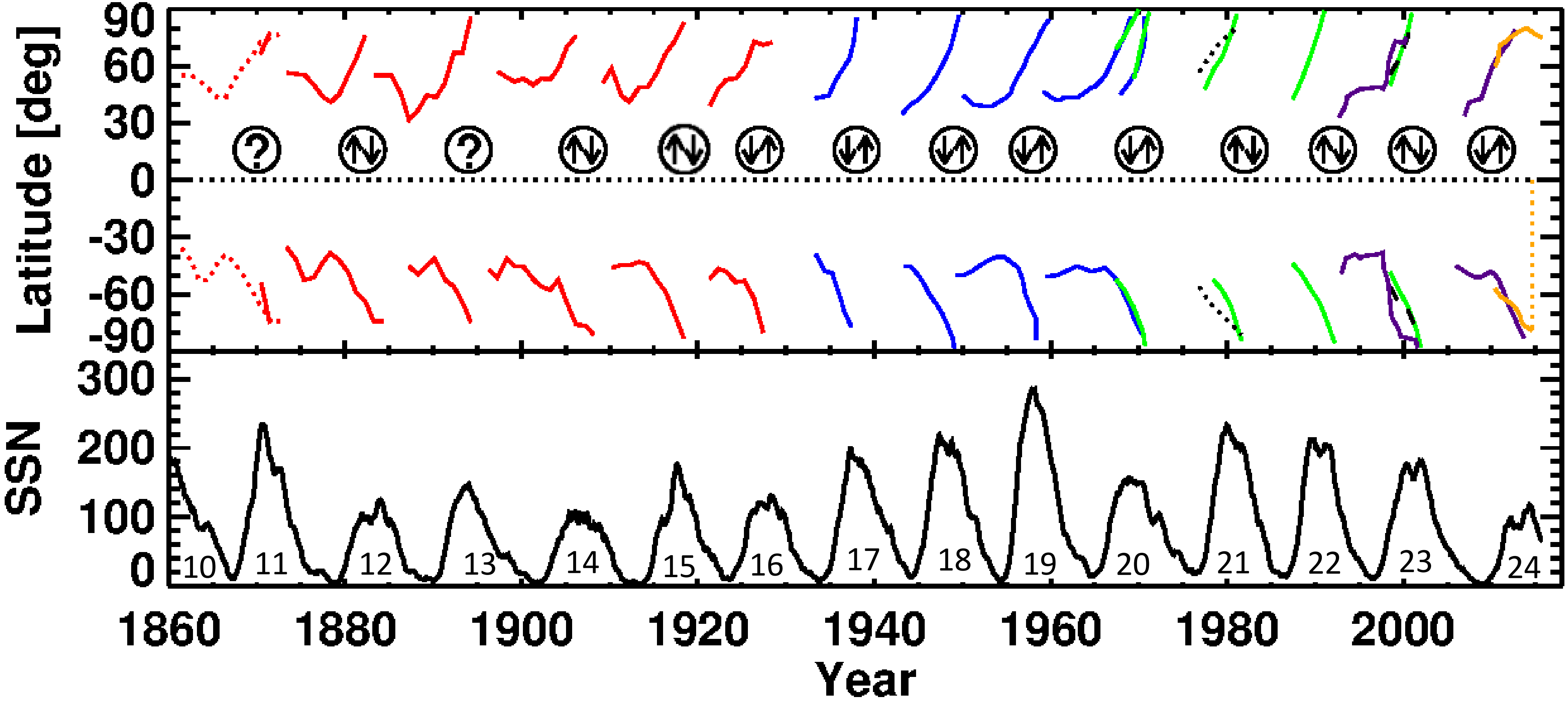

Magenta: PE from NoRH
Orange: PE from SDO
…… Fujimori 1984
------ Pojoga & Huang 2003

10-20: Stix (compiled from Lockyer 1931; Kiepenhauer 1953; Waldmier 1968; 1973)
20-23: Lorenc et al. (2003)
23-24 Gopalswamy et al. 2003; 2012; 2016

Gopalswamy et al. 2018 JASTP

Cycle 16 has similar RTTP behavior as cycle 24; the reversal asymmetry also changes

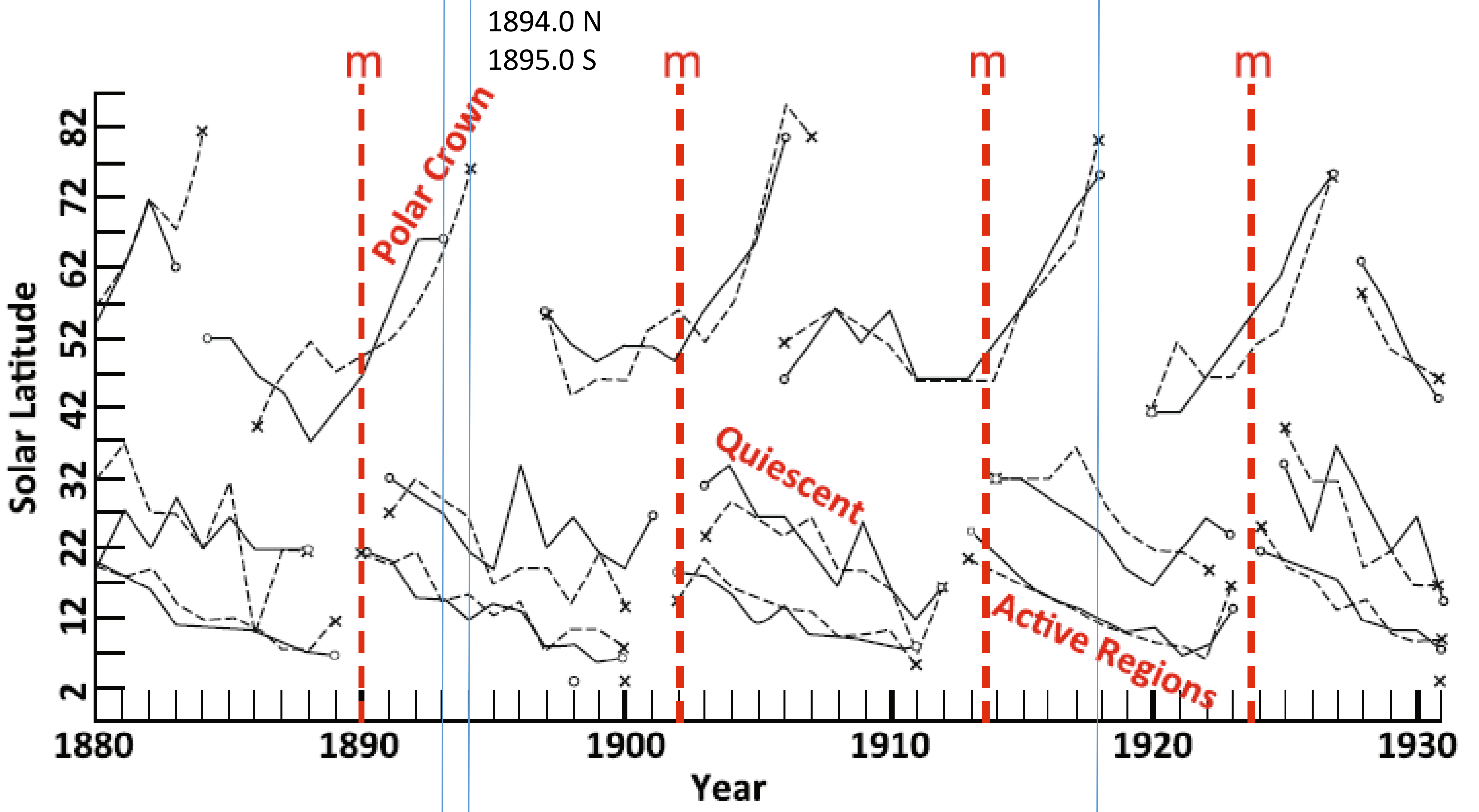

Bocchino 1933 in Cliver 2014; also Evershed & Evershed 1917 (Kodaikanal)

Historical RTTPs

Reversal asymmetry changes every 3-5 cycles
Extended period of HL Prominences in cycle 16, 20 maxima

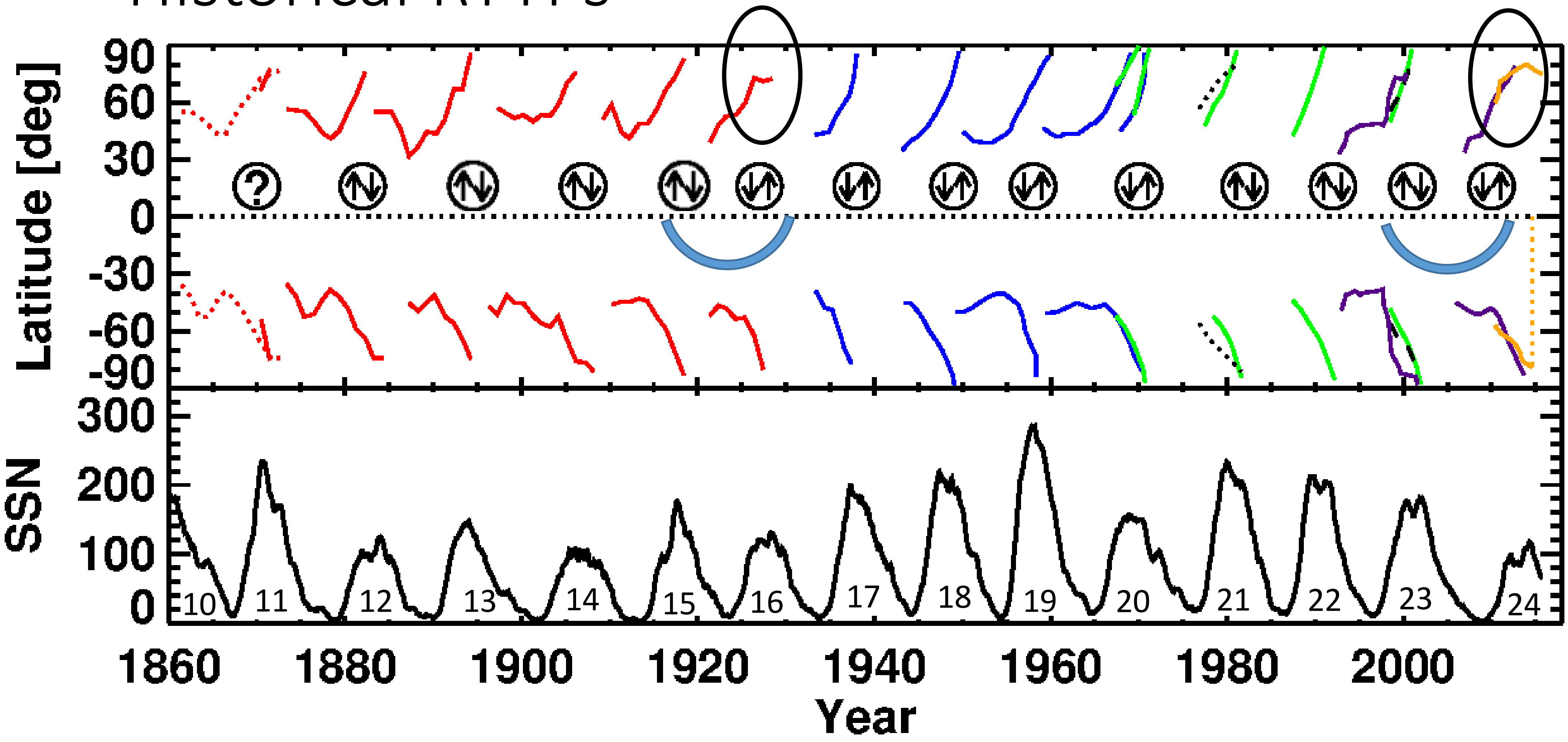

Magenta: PE from NoRH
Orange: PE from SDO
…… Fujimori 1984
------ Pojoga & Huang 2003

10-20: Stix (compiled from Lockyer 1931; Kiepenhauer 1953; Waldmier 1968; 1973)
20-23: Lorenc et al. (2003)
23-24 Gopalswamy et al. 2003; 2012; 2016

Gopalswamy et al. 2018 JASTP

Cycle 16 has similar RTTP behavior as cycle 24; the reversal asymmetry also changes

Summary

- CMEs are known only since the 1970s
- In hindsight, we see that they are responsible for historical magnetic storms and particle events
- CMEs originate in closed field regions (sunspot, filament)
- CME rate – SSN correlation is weak during the maximum phase because of mid & high latitude CMEs not related to sunspots
- Unusual polar conditions prevailed in the north polar region of the Sun until recently (extended eruptive activity, low polar Tb, B~0)
- A similar situation prevailed in cycle 16
- In cycles 24 and 16, the reversal asymmetry switched from NS to SN
- In 14 cycles, there were three switches, indicating a 3-5 cycle periodicity
- The switch in reversal asymmetry can be attributed to wrong-polarity surges

OSO-7 CMEs

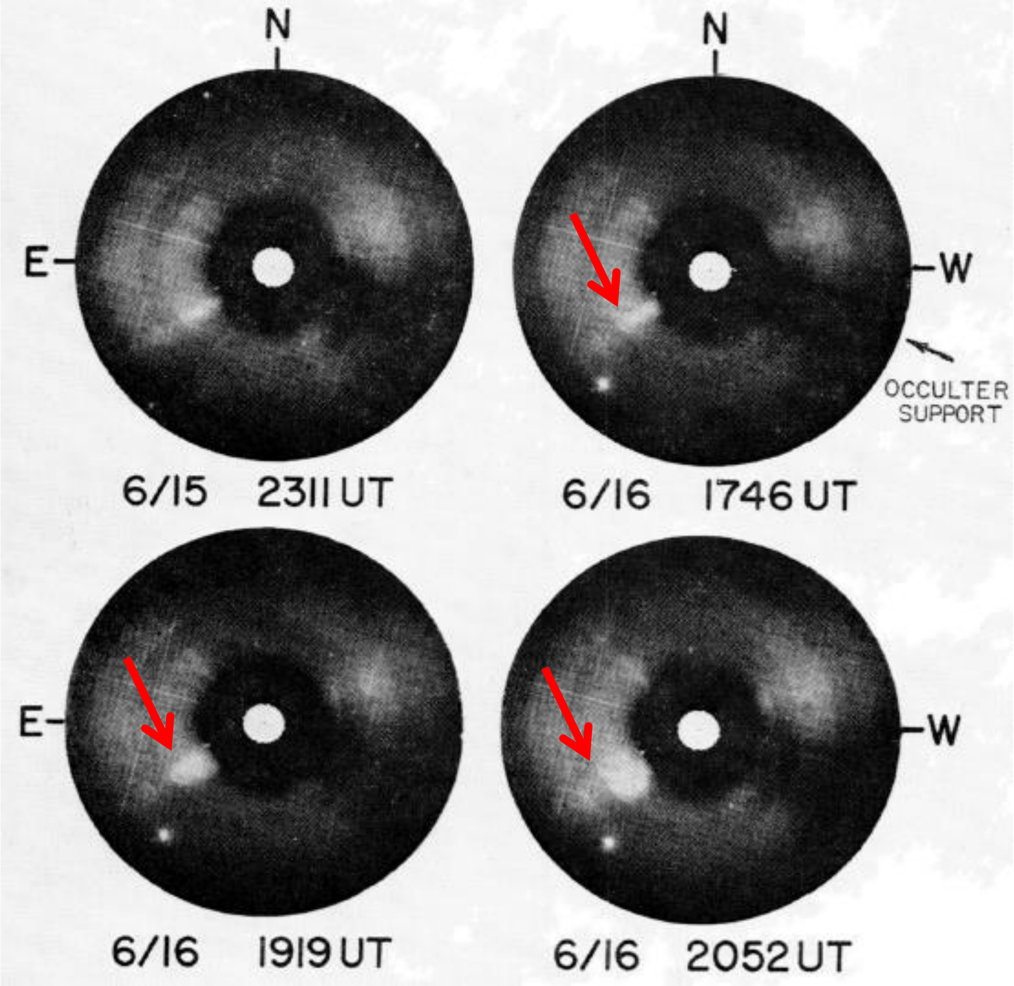

Koomen et al. 1974 made the connection to Gold bottle

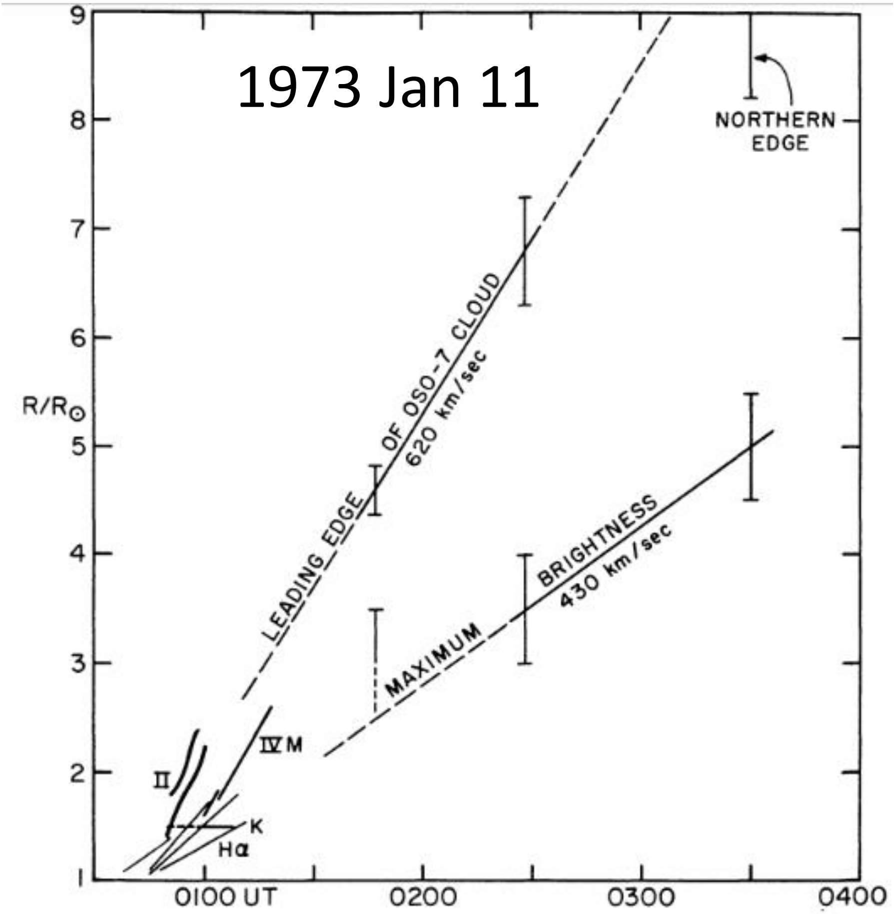

Stewart et al. 1974

Type II burst from the leading shock

Type IV burst immediately behind the CME

Eruptive prominence deep inside the CME

A Skylab CME: “new-found cosmic phenomenon”

coronal transient → coronal mass ejection

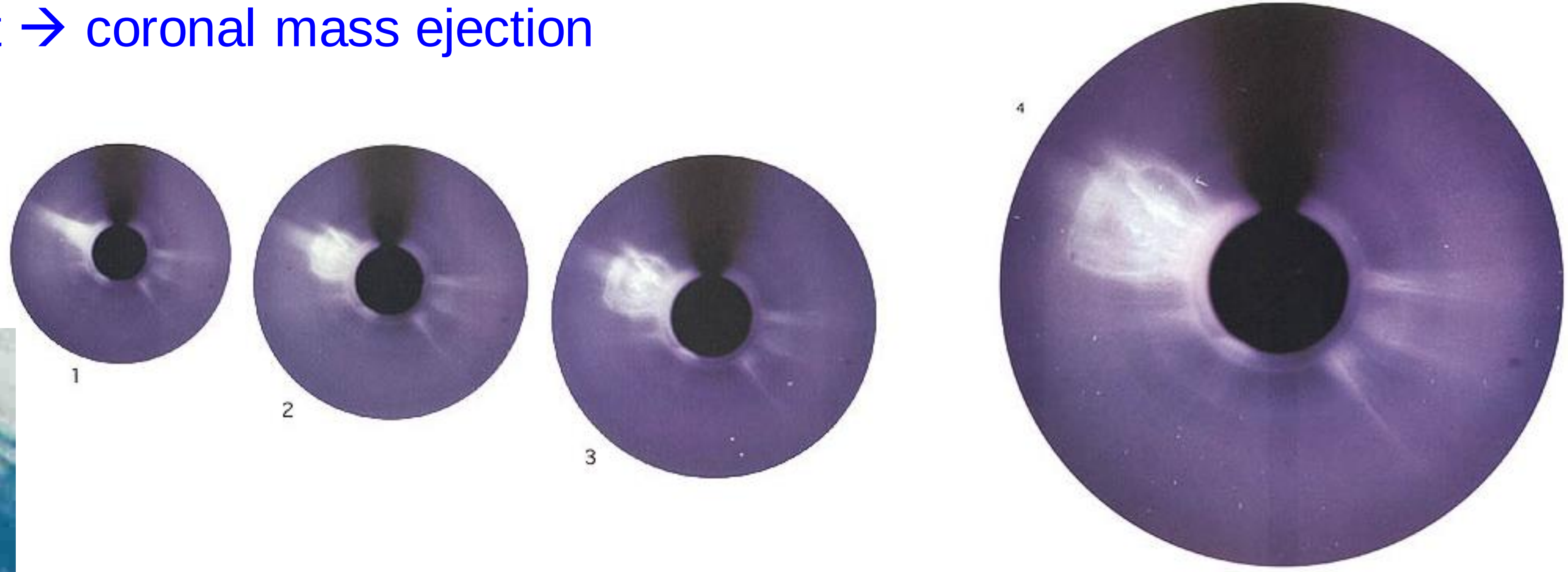

Skylab ATM Coronagraph
May 1973 - Feb 1974
110 CMEs observed in 227 days

Speed: 725 km/s

Solwind (P78-1)

1607 CMEs

2/24/1979 to 9/13/1985

Halo CMEs (Howard et al. 1982)
All but 2% of IP shocks had CME association (Sheeley et al. 1985)
High-latitude CME (Sheeley et al. 1980)
Solar Cycle Variation (Howard et al. 85)
Acceleration of slow CMEs and Deceleration of fast CMEs

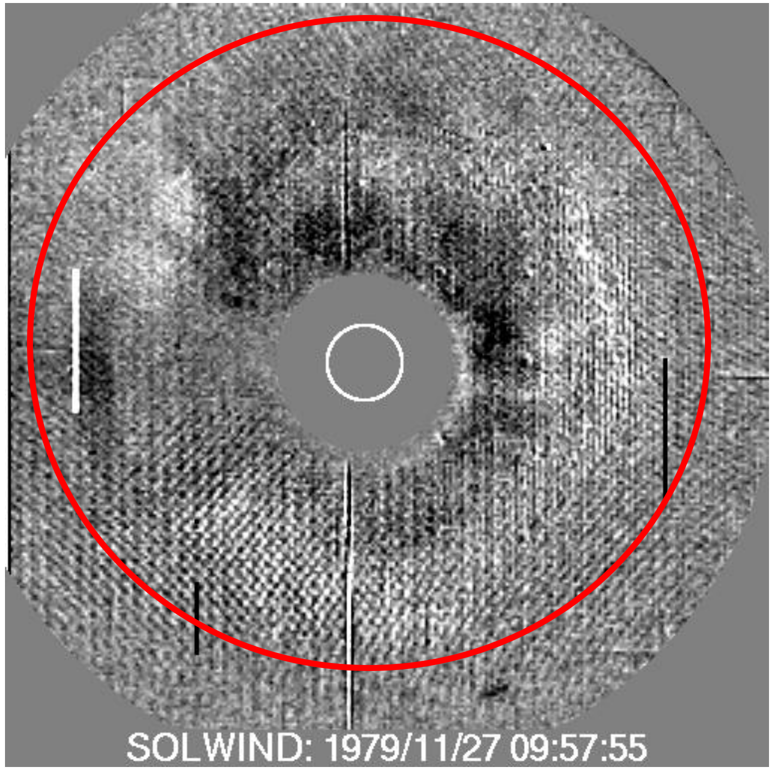

Howard et al. 1982

This CME reached HELIOS-1 (0.84 AU) ~ 61 hours later on July 5 at 15:00 UT

PVO and HELIOS were occasionally in quadrature with SOLWIND. Helped quantify IP acceleration

Lindsay et al. 1999; Gopalswamy et al. 2001

SMM Coronagraph/Polarimeter

1206 CMEs

SMM 1980-1989

Emphasis on filament eruption CMEs
CME latitudes similar to prominence lat. rather than flare latitudes
Three-part CMEs (Hundhausen 1993)
No Halo CMEs; lowest average speed (quadrant FOV)
Close to the Sun – CMEs still accelerating (Howard et al. 1987)

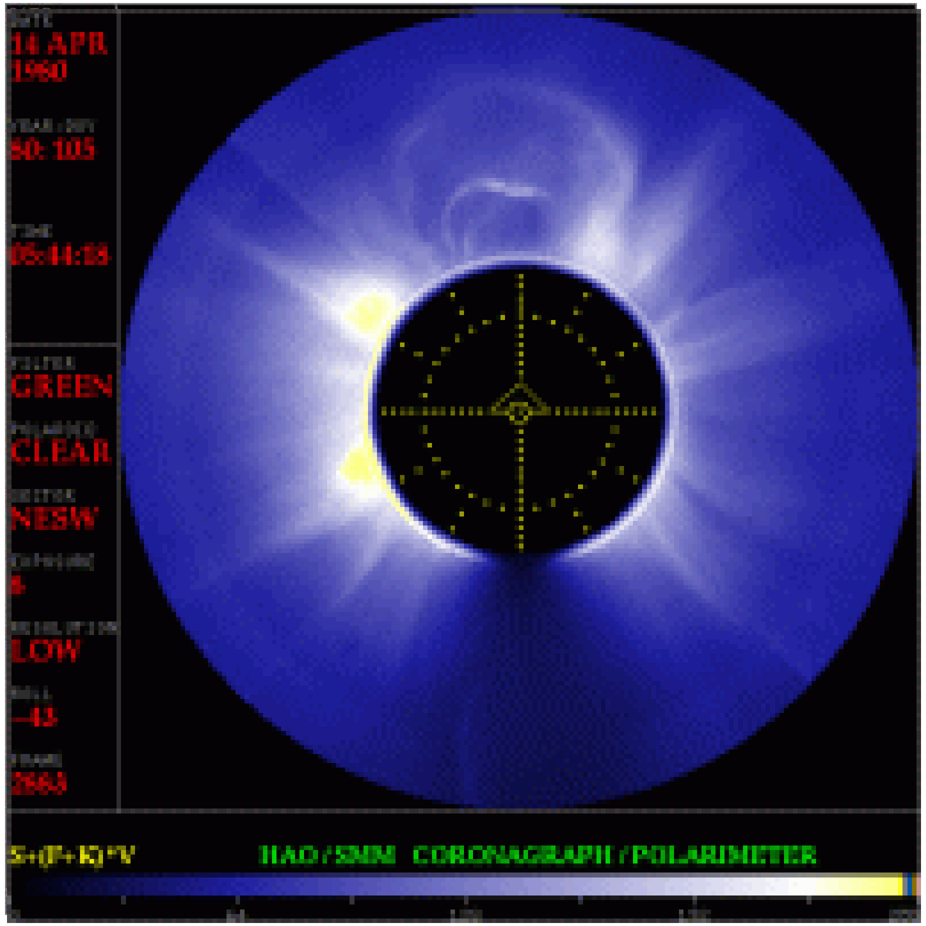

9-17 April 1980 HAO

The crew of STS-41-C (space shuttle Challenger) captured, repaired and redeployed SMM in April 1984

Astronauts Nelson and van-Hoften replaced the satellite's attitude control mechanism and the main electronics box of the coronagraph.